Influence of post-Tehuano oceanographic processes in the dynamics of the CO_2 system in the Gulf of Tehuantepec, Mexico

Authors:

Cecilia Chapa-Balcorta[1,2,3], J. Martin Hernandez-Ayon[2 *], Reginaldo Durazo[1,4], Emilio Beier[5], Simone R. Alin[6], Andrés López-Pérez[7].

Author affiliations:

[1]Facultad de Ciencias Marinas, Universidad Autónoma de Baja California, Apdo. Postal 453, Ensenada, Baja California, México.

*[2]Instituto de Investigaciones Oceanológicas, Universidad Autónoma de Baja California, Apdo. Postal 453, Ensenada, Baja California, México. *E-mail: jmartin@uabc.edu.mx*

[3]Universidad del Mar. Ciudad Universitaria SN. CP 70902. Puerto Ángel Oaxaca, México.

[4]Profesor Invitado, Instituto Politécnico Nacional, Centro Interdisciplinario de Ciencias Marinas, Apdo. Postal 592, La Paz, Baja California Sur, México.

[5]Centro de Investigación Científica y de Educación Superior de Ensenada, Unidad La Paz, Baja California Sur, México.

[6] Pacific Marine Environmental Laboratory, National Oceanic and Atmospheric Administration, Seattle, WA 98115 USA, simone.r.alin@noaa.gov

[7]Departamento de Hidrobiología, Universidad Autónoma Metropolitana Unidad Iztapalapa. San Rafael Atlixco No. 186, Col. Vicentina, Iztapalapa, 09340, Distrito Federal, México.

Corresponding author

Instituto de Investigaciones Oceanológicas

Universidad Autónoma de Baja California

jmartin@uabc.edu.mx

Key Points

1. The aragonite saturation horizon is close to the surface near the coast.
2. Reported air-sea CO_2 fluxes are the largest observed to date in the Mexican Pacific.

Abstract

This investigation reports, for the first time, results of CO_2 system variables in the Gulf of Tehuantepec, located in the Mexican tropical Pacific. We quantified the post-Tehuano concentration of dissolved inorganic carbon (DIC) and pH (April 2013). These values were used to calculate pCO_2, aragonite saturation (Ω_{Ar}) and air-sea CO_2 fluxes (FCO_2). The intense vertical stratification was found to contribute to the biogeochemical processes in surface waters (< 70 m). However, in post-Tehuano conditions, high pCO_2 (~1000 µatm) and DIC concentrations (2200 µmol kg^{-1}), as well as low Ω_{Ar} (~1.1) and pH (~7.5) remain in surface waters for a few days after Tehuano winds have weakened. We identified four oceanographic areas: a) a highly mixed region due to previous Tehuano events; b) coastal upwelling in the western region; c) mesoscale eddies; and d) a poleward surface coastal current. The first three promoted the influence of Subtropical Subsurface Water in the chemistry of surface waters, whereas the coastal current contributed to the horizontal advection of DIC. The calculated CO_2 fluxes ranged from -2.3 mmol m^{-2} d^{-1} in areas with stratified waters, to over 25 mmol m^{-2} d^{-1} for mixed areas. Positive values indicate an ocean-to-atmosphere flux. Our findings suggest that the Gulf of Tehuantepec is a major source of CO_2 into the atmosphere.

Index Terms: Eastern Tropical Pacific, Ocean Acidification, Tehuano gap winds, carbonate system, mesoscale structures, carbon fluxes.

1 Introduction

Approximately 50% of the CO_2 that is absorbed in the subtropical region of the Pacific Ocean returns to the atmosphere in the tropics [*Feely et al.*, 1997; *Ishii et al.*, 2014]. Variations in the concentration of dissolved inorganic carbon and air-sea CO_2 fluxes in the tropical ocean are both enhanced by high CO_2 levels in subsurface water. These, in turn, are regulated by dynamic processes derived from wind forcing, such as coastal upwelling events, thermal fronts and mesoscale eddies, among others [*Chen et al.*, 2007; *Friederich et al.*, 2008; *Wang et al.*, 2006].

In the Gulf of Tehuantepec (GoT), intermittent northerly winds, called “nortes” or “Tehuanos” (speed above 10 m s^{-1}) result from pressure gradients between the Gulf of Mexico and the GoT from November to March [*Barton et al.*, 1993; *Trasviña et al.*, 1995]. These winds produce strong changes in the structure of the water column and a complex coastal circulation. Under the influence of Tehuanos, surface water flows offshore, which causes mixing and entrainment of subsurface water. The result is a temperature drop of up to 8 °C at the center of the GoT, and the formation of a cold water plume that may stretch over 400 km offshore and be more than 200 km wide [*Barton et al.*, 1993; *Trasviña et al.*, 1995].

Wind relaxation after Tehuanos results in the formation of mesoscale structures [*Barton et al.*, 2009; *Chang et al.*, 2012]. The most frequent structure is an anticyclonic eddy at the

GoT western region [*Barton et al.*, 2009; *Willett et al.*, 2006], which can last several months. Also reported is the presence of a cyclonic eddy in the eastern/central GoT, as well as a coastal current to the east that travels north/northwest parallel to the coast [*Barton et al.*, 2009; *Velázquez-Muñoz et al.*, 2011]. Once the Tehuano season is over, during May-June [*Romero-Centeno et al.*, 2007] the GoT becomes highly stratified, displaying a strong pycnocline [*Fiedler et al.*, 2013], mesoscale structures, and coastal-trapped waves related to baroclinic instabilities [*Flores-Vidal et al.*, 2014].

The importance of mesoscale structures lies in their effect on the vertical distribution of chemical properties, particulate inorganic and organic matter, heat, mass, and living organisms and their transport offshore [*Adams and Flierl*, 2010; *Chierici et al.*, 2005; *Samuelsen and O'Brien*, 2008]. Anticyclonic eddies, for example, deepen the pycnocline by Ekman pumping, and therefore keep subsurface waters that are DIC-rich, with low pH and near-undersaturated aragonite levels, away from the surface. The opposite is true when cyclonic eddies occur and eddy-induced upwelling transports subsurface waters toward the surface.

In the Gulf of Tehuantepec, water masses in the upper 500 m are composed primarily of Tropical Surface Water (TSW) and Subtropical Subsurface Water (StSsW) [*Barton et al.*, 2009; *Fiedler and Talley*, 2006]. StSsW (Table 1) contains part of the oxygen minimum layer (OML) and the maximum dissolved inorganic carbon (>2200 μmol kg^{-1}) [*Franco et al.*, 2014]. The upper depth limit of this water mass ranges between 70 and 100 m; therefore, it could have a significant influence on the biogeochemical processes in GoT surface waters when mesoscale structures, heavy mixing, or upwelling occur. For this region of the Pacific Ocean, the depth distribution of these water masses has been reported to depend, to a greater or lesser extent, on seasonal variations of the oceanic circulation [*Godínez et al*., 2010].

Due to the presence of intense north winds, few in-situ oceanographic studies have been conducted in this region. Hence, current knowledge on carbon biogeochemistry in the GoT is scarce. To date, there are no published studies on the CO_2 system in this region. The Tehuano and post-Tehuano conditions are expected to lead to an increase in DIC concentrations and a decrease in pH of surface water accordingly. Furthermore, the magnitude of air-sea fluxes of CO_2 in the region remains unknown. Based on studies of other tropical regions in the Eastern Tropical Pacific (ETP), the Gulf of Tehuantepec is expected to be a source of CO_2 to the atmosphere [*Franco et al.*, 2014; *Paulmier et al.*, 2008].

Ecologically important coral species such as *Pocillopora damicornis, P. meandrina* and *Porites Panamensis* live in the coastal areas of the GoT [*López-Pérez et al.*, 2014] . Aragonite saturation state variability may affect corals and other calcifying species such as coccolithophorids and foraminifera [*Müller et al.*, 2010; *Rixen et al.*, 2012]. However, no published information is available on the carbon chemistry conditions in which calcifying organisms live. The present study provides the first quantitative information on the CO_2 system in the Gulf of Tehuantepec. The oceanographic and biogeochemical data collected under post-Tehuano conditions show the effects of oceanographic conditions on the vertical distribution of carbon variables across the water column that impact surface carbon fluxes and the depth of the aragonite saturation horizon. Due to the strong variability in oceanic and atmospheric conditions, the GoT might be considered as a natural laboratory for investigating the CO_2 system.

2 Methods

2.1 Sample and data collection

Sampling was carried out during an oceanographic cruise led by the Mexican Navy (Secretaría de Marina) aboard RV *Altair* (Figure 1). Data on temperature, conductivity and pressure were recorded to a maximum depth of 500 m at 26 stations using a factory-calibrated Seabird SBE19 CTD. From these data, salinity (PS-78) and density (EOS-80) were calculated.

At each station (Figure 1), water was collected at nine depths using 5 L Niskin bottles attached to a hydrographic wire. Sampling depth was calculated from the cable length, using a cable counter, and the line angle, using an inclinometer). Water samples were stored in 500 mL sodium borosilicate bottles and preserved with 100 µL of $HgCl_2$ saturated solution. Afterwards, bottles were sealed with Apiezon™ grease to prevent evaporation and contact with the atmosphere.

The concentration of dissolved inorganic carbon (DIC) was measured using the coulometric method described by *Johnson et al.* [1987]. Certified reference material (CRM) from Dr. Andrew Dickson's laboratory at Scripps Institution of Oceanography, University of California, San Diego, was used for assessing the precision and accuracy of measurements. The reference material gave a relative difference averaging 2.2 ± 1.1 μmol kg^{-1}, with a maximum of 4 μmol kg^{-1} (0.2% error) with respect to the certified value.

The pH was measured using a glass electrode with an Orion potentiometer at 25 °C. The electrode slope was calculated 24 hours before the analysis using NBS buffers of pH 7.01 and 4.01; afterwards, the electrode was kept immersed in filtered seawater. The reference material mentioned above was used as a seawater pH standard. The pH value in the seawater scale from the certified reference material was calculated with the CO2SYS program using the certified DIC and TA values [*Lewis and Wallace*, 1998]. The millivoltage of the reference material was recorded at the beginning and end of each session. All measurements were performed at 25 °C in the seawater scale (pHsw).

The aragonite saturation state (Ω_{Ar}), pH_{sw}, and pCO_2 at in-situ temperature, salinity and pressure were calculated with the CO2SYS program [*Lewis and Wallace*, 1998] adapted for Matlab by *Van Heuven et al.* [2009], using discrete DIC and pH_{sw} measurements (25 °C). The dissociation constants proposed by *Lueker et al.* [2000] were used for this purpose. This resulted in a precision of ± 0.04 units for pH_{sw} in situ, ± 0.2 units for Ω_{Ar} and ± 56 μatm for pCO_2. The uncertainty for pCO_2 is higher than what would be obtained with the TA-DIC combination; however, the pCO_2 range of variability observed was 28 times greater than the error, and hence our measurements are representative of the processes taking place in the GoT.

The air-sea CO_2 flux (FCO_2) (mmol C m^{-2} d^{-1}) was calculated as:

$$FCO_2 = kK_o(pCO_{2w} - pCO_{2a}) \quad (1)$$

where k is the gas transfer velocity, which is a function of wind speed, calculated according to [*Wanninkhof*, 1992]; the coefficients used were 0.31 and 0.39 for weak (<6 ms^{-1}) and strong (>6 ms^{-1}) wind speeds, respectively; K_o is the aqueous-phase solubility of CO_2 in seawater at in situ temperature and salinity, calculated using the equations of *Weiss [1974]*; pCO_{2w} and pCO_{2a} are the CO_2 partial pressure in water and air, respectively. This calculation used the average atmospheric pCO_2 of 398.35 μatm reported for April 2013 by the Mauna Loa observatory (ftp://aftp.cmdl.noaa.gov/). Wind speed data (m s^{-1}) were obtained from daily NOAA SeaWinds satellite images with a spatial resolution of 0.25 degrees [*Zhang et al.*, 2006a; *Zhang et al.*, 2006b]. The calculated error for FCO_2 was ± 0.5 mmol m^{-2} d^{-1} for winds $\leq$ 2.5 m s^{-1} (this condition prevailed throughout the sampling campaign), with a peak of 1.3 mmol m^{-2} d^{-1} for high-speed winds (4 m s^{-1}).

The stratification was calculated with the method of *Simpson and Bowers* [1981] for the upper 300 m. Wind data were obtained from daily composite NOAA SeaWinds satellite images (www.ncdc.noaa.gov) with a spatial resolution of 0.25 degrees. Wind stress was calculated according to *Large and Pond* [1981]. Mesoscale eddies were identified visually using satellite images of the sea level anomaly (SSHa) (http://www.aviso.oceanobs.com/duacs/). These data consist of interpolated daily images resulting from multi-satellite (2 to 4 satellites) observations of 10- to 30-day cycles for the same period of hydrographic observations, and with the same spatial resolution as wind data. Geostrophic speed and dynamic height were calculated using a no-motion reference level of 300 dbar. This level adequately represents the surface circulation and was applied by *Barton et al.* [2009] and *Flores-Vidal et al.* [2014] for the same region.

3 Results

3.1 Water masses

In line with previous studies for this region [*Barton et al.*, 2009; *Fiedler and Talley*, 2006], the water masses observed in the first 500 m depth were the TSW and StSsW (Figure 2). TSW is distributed mainly from the surface layer down to the 18°C isotherm, where the StSsW starts (Figure 2a). In this layer, TSW showed low DIC concentrations (1923-2050 µmol kg^{-1}) and low pCO_2 values (276-648 µatm, not shown) compared with subsurface water (Figure 2c). StSsW showed higher DIC concentrations, ranging between 2200 and >2270 µmol kg-1 (Figure 2c). The depth of the upper boundary of the DIC-rich StSsW water mass varies throughout the study area as a reflection of the dominant physical processes in each region. In regions dominated by anticyclonic eddies, StSsW was observed at approximately 100 m depth, whereas in regions of cyclonic circulation it occurred at less than 30 m. In areas with the highest vertical mixing resulting from previous Tehuano events, this water was found near the surface (Figure 2a). Consequently, the rise and/or upwelling of StSsW is expected to enrich surface water with DIC. This process is described below in terms of the physical dynamics that take place after an intense north wind event.

3.2 Post-Tehuano conditions

Prior to the sampling period, five wind events with speed greater than 10 m s^{-1} occurred between March and the first week of April 2013; the most intense reached 19.8 m s^{-1} during the first week of March (Figure 3a). These exerted a strong wind stress on the sea surface (Figure 3b) and declined gradually to post-Tehuano conditions (Figure 3c). During the April sampling under post-Tehuano conditions, winds fluctuated between ~2 and 5 m s^{-1}

and caused a minor forcing (Figure 3c), which nonetheless was of sufficient intensity to produce coastal upwelling areas in the eastern and western ends of the GoT (Figure 3c). The combination of strong winds and subsequent calm led to different oceanographic conditions: the coastal region displayed a highly mixed zone and another area with upwelling; mesoscale eddies and a poleward coastal current were also identified. Accordingly, the distribution patterns of CO_2 variables were directly associated with the various oceanographic conditions. Each of these conditions and their effect on the chemistry of the CO_2 system are described below.

3.2.1 Coastal upwelling

Westerly winds (~0.03–0.04 N m^2) flowing parallel to the GoT west coast were recorded during the sampling campaign (six days), (Figure 3c). These caused an Ekman transport of 75–96 m^3 s^{-1} 100 m^{-1} (calculated as per *Schwing et al.* [1996] for the average stress over the six days) and a rise of isopycnals in the first 60 km from the coast (transects I and II, Figures 4-Ia and IIa), with an ascension of water from 60 m up to 20–30 m, as noted in figures. The water flowed with the highest geostrophic speed observed in all the study area (53 cm s^{-1}, Figure 4-Ib). The importance of this finding lies in that previous studies have focused only on the effect of processes directly derived from intense Tehuano winds, omitting information related to the fact that upwelling events are also formed in this region. Coastal upwelling events promote an ascent of subsurface water, leading to changes in DIC concentrations, pH values and Ω_{Ar}, and may cause significant changes in the air-sea flux of CO_2. At 30 m depth near the coast (6–20 km), DIC levels of 2150 μmol kg^{-1} were recorded, as well as 2224 μmol kg^{-1} in transects I and II, respectively (Figures 4-Ic and 4-

IIc). High DIC concentrations were due to a greater influence of StSsW. Minimum pH and Ω_{Ar} values (Figure 4-IId-e) were observed just 6 km off the coast at depths where peak DIC concentrations were recorded. Similar to the above variables, the aragonite saturation horizon (Ω_{Ar} = 1) rose 100 m in just 100 km, reaching a depth of 28 meters near the coast (Figure 4-Ie and 4-IIe). Moreover, pCO_2 values increased to levels as high as 1900 µatm (Figure 4-If).

3.2.2 Area of intense vertical mixing

An area of intense vertical mixing was detected in the central region of the Gulf of Tehuantepec. Although wind stress was relatively low during sampling, five strong wind events in the previous days recorded mean wind stress values of ~0.15 N m^{-2} (Figure 3b). Vertical mixing and reduced stratification (634 J m^{-3}) resulting from these wind events were detected during the sampling conducted two weeks later. The fact that the upper StSsW limit (Figure 2) is represented by the 25.5 kg m^{-3} isopycnal suggests that this DIC-rich water mass was closer to the surface. The stations near the coast showed the highest subsurface DIC concentrations and lower pH, 2218 µmol kg^{-1} and ~7.7, respectively (Figure 4-III), along with pCO_2 values of 1750 µatm (Figure 4-IIIf). Besides, just 80 km off the coast, the aragonite saturation horizon was observed 160 m above the depth where it occurs 120 km offshore (190 m).

3.2.3 Mesoscale eddies

Two anticyclonic eddies were recorded: one in the Gulf of Tehuantepec (A1) and another to the east of it (A2) (Figure 5). The sequence of daily altimetry images between March and April (not shown) suggests these structures resulted from Tehuano and Papagayo winds, respectively. Likewise, altimetry data pointed to the presence of two cyclonic eddies localized in the GoT at the beginning of the sampling period. Only the central cyclonic eddy was observed during the sampling period (C1). As detailed below, anticyclonic eddies promoted the sinking of the aragonite saturation horizon and the pH, pCO_2, and DIC isolines; the opposite occurred in association with cyclonic eddies.

The cyclonic eddy in the center of the GoT (C1) was adjacent to the coast and stretched down to 300 m, as evidenced by the temperature distribution in section III of Figure 4. Within this cyclonic eddy, DIC-rich water ranged from 20 down to 200 m. Similarly, pH values were 7.7 and 8.1 at the bottom and surface, respectively. Aragonite saturation and pCO_2 fluctuated from 0.9 to 4.2, and from 1752 to 289 μatm, respectively, following the same variation pattern as DIC. In the eastern portion of the cyclonic eddy (Figure 4, transect IV,), sampled on April 14-15 when it occupied most of the GoT, more pronounced isotherm slopes were observed, particularly near the coast. This resulted in a better definition of cyclonic circulation, with currents flowing to the west (poleward) near the coast and to the east (equatorward) from 100 km offshore. The depth of isotherms (isopycnals) was minimal at the center of the eddy. Consequently, a higher DIC concentration relative to the coastline and offshore was observed. Along the coastline, the DIC-rich StSsW carried waters of relatively low pH (~7.6), and a shallower saturation horizon (~30 m) was evident close to the coast. These values show that this eddy caused a slight rise of StSsW, with the consequent DIC enrichment.

On the eastern edge of the Tehuantepec anticyclonic eddy measured during the cruise, isotherms and isopycnals sank down to 50 m, with a current of ~30 cm s^{-1} (Figure 4, sections I a-f and II a-f, stations located away from the coast). This led to the sinking of the aragonite saturation horizon and isolines of pH 7.6 and DIC 2200 µmol kg^{-1}, which were >80 meters deeper than in the more coastal station, with peak values of pH and Ω_{Ar} in the eddy region (Figure 4, section I d-e). Furthermore, pCO_2 values ranged between 400 and 1180 µatm between 100 and 120 km off the coast, and the aragonite saturation horizon was found between 120 and 200 m depth. The accumulation of surface water within the anticyclonic eddy facilitated the stratification of the water column (1418 J m^{-3}), this being the maximum value recorded for the study area.

The influence of the Papagayo eddy was evident in section V. The depth of the thermocline increased in the three stations farther away from the coast compared to the rest of the transect, while it occurred at a depth of only 10 m near the coast. DIC-rich water (2200 µmol kg^{-1}, pH 7.6) was located at ~70 m depth at the station closest to the center of this eddy (Figure 4 section V, oceanic stations).

The changes observed in the CO_2 system resulting from mesoscale eddies suggest that these structures may have a significant effect on biogeochemical and ecological processes in the region. Mesoscale eddies occur throughout the year, being more frequent during the Tehuano season [*Willett et al.*, 2006]; hence, their effects on the CO_2 system could be apparent throughout the year.

3.2.4 Coastal current

The data obtained in transects I-V, as well as the maps of geostrophic velocity derived from altimetry, reveal a poleward coastal flow (4.4 cm s^{-1}). Temporal coverage of data used in this study is not enough to discern whether this flow is a constant current or derives from eddy rims associated mainly with cyclonic eddies (Figure 4). Previous studies refer to a poleward coastal current detected at the same region during winter, spring and summer [*Barton et al.*, 2009; *Flores-Vidal et al.*, 2011; *Trasviña and Barton*, 2008; *Willett et al.*, 2006] ;[*Velázquez-Muñoz et al.*, 2011]. Furthermore, geostrophic velocity in section I (Figure 4) indicates a poleward subsurface flow in spite of the coastal upwelling and the anticyclonic eddy. Therefore, we assume the poleward flow observed in this study is the same structure reported in the literature. The core of this current was between the 100 and 180 m, i.e. StSsW. Given its characteristics, this current was associated with a higher DIC concentration, lower pH and lower Ω_{Ar}, and was more corrosive than water from the same depth collected offshore, except for sections IV and V, where the DIC concentration near the coast was similar to or higher than in the rest of the water column.

3.2.5 Surface distribution

The surface distribution of the variables studied reflects the effect of the oceanographic conditions described in the previous sections (mixing, upwelling, eddies, coastal current). σ-θ shows the surface maxima near the coast in the highly mixed region (Figure 6a, 16°45' N, 96° W) associated with the cyclonic circulation that promotes the rise of subsurface water and the redistribution of mixed water, leading to CO_2 enrichment. In contrast, regions dominated by anticyclonic circulation showed a deepening of low-density isopycnals (Figure 6). Surface DIC concentrations, directly related to waters of lower density, ranged between 1923 and 2218 µmol kg^{-1} (Figure 6b), coupled with a higher pH (Figure 6c); these were located at 14°30'–15° N and 97°–97°30' W, (Figure 6b). Separately, Ω_{Ar} of the upper layer (not shown) ranged between 1.1 and 4.3. Peaks were associated with the most stratified region, and minimum levels were recorded in the region with the highest mixing and upwelling. The 20 m depth was dominated by a highly mixed region (15°30' N, 95°45' W) and the dome of the central cyclonic eddy (C1, Figures 5 and 6) (15°15' N, 96°30' W, Figure 6d), with DIC >2200 µmol kg^{-1} and low pH (Figure 5e, f); minimum values were observed in the area most affected by the Tehuantepec anticyclonic eddy (A1).

3.2.6 Air-sea flux of CO_2

The increase in DIC concentration in surface waters translated into high calculated fluxes of CO_2 into the atmosphere (Figure 7), which ranged between -2.3 and 42 mmol C m^{-2} d^{-1}. Peak values were observed in the highly mixed area (42 mmol C m^{-2} d^{-1}), whereas a flux of 5 mmol C m^{-2} d^{-1} was estimated in the coastal upwelling region. Separately, the regions under the influence of anticyclonic eddies displayed a flux indicating near-equilibrium with the atmosphere. The rest of the region dominated by cyclonic circulation displayed low fluxes into the ocean of -2.6 mmol C m^{-2} d^{-1}. The intense air-sea fluxes in the mixed area which resulted from previous wind and upwelling events confirm that the GoT may be a source of CO_2 into the atmosphere during the entrainment of subsurface waters, due to the turbulent mixing driven by the wind. The results shown represent what remains after the last Tehuano event ended, and wind speeds fell below 5 m s^{-1}. Such high fluxes are driven by a strong air-sea DIC gradient and these post-Tehuano DIC fluxes may remain for several days after a strong wind event. Air- sea fluxes may be larger during Tehuano events when wind stress breaks the interface and increases gas exchange. Considering that the Tehuano wind season lasts approximately four months, the Gulf of Tehuantepec represents an important source of CO_2 in the Eastern Tropical Pacific, likely being the most important area reported so far for the Mexican Pacific.

4 Discussion

This paper describes the development of post-Tehuano conditions during April 2013 and the consequent spatial variation in the CO_2 system. The greatest wind forcing occurs during the Tehuanos season from November to March [*Trasviña et al.*, 1995]. However, April can be considered as a transitional month, a post-Tehuano condition where the wind drops to ~3–5 m s^{-1}. Four oceanographic conditions were identified in the Tehuantepec region during the post-Tehuano period: 1) a highly mixed coastal region; 2) mesoscale eddies; 3) a coastal upwelling in the western region; and 4) a coastal current (Figure 8). This section discusses how these conditions impacted the CO_2 system, as well as their importance and ecological implications.

4.1.1 Vertical mixing

The water column near the coast and in the center of the study area (Figure 4, coastal stations in transects III and IV) showed the greatest impact of wind during previous Tehuano events. The highest surface DIC and pCO_2 concentrations, together with the greatest flux of CO_2 into the atmosphere and minimum surface pH and Ω_{Ar} are expected under this scenario. According to *Trasviña et al.* [1995], vertical mixing is the process that leads to the greater thermal anomalies after Tehuano events, since the mixed layer expands almost immediately after the onset of a strong wind event. *Flores-Vidal et al.* [2014] show in their figure 6 that water at 60 to 70 m depth can be transported to the surface as a result of a strong wind. When the wind weakens, the region with the lowest vertical stratification is confined to the coast, near the head of the gulf. In this work, the mixed area is evidenced by the 54% reduction of stratification (784 J m^{-3}) compared to the maximum stratification within the Tehuantepec anticyclonic eddy (1414 Jm^{-3}), typical of the tropical region [*Fiedler et al.*, 2013].

In this region, surface DIC concentrations exceeded 2200 µmol kg^{-1} and pCO_2 levels were above 1600 µatm. These figures show higher values than those recorded in other regions of the North Eastern Tropical Pacific (NETP) influenced by StSsW (1290-1340 µatm [*Franco et al.*, 2014]), similar to the coastal region from Colima to Michoacan, and slightly lower than DIC concentrations reported for the Midriff Islands region in the Gulf of California (~2270 µmol kg^{-1}) [*Hernandez-Ayon et al.*, 2013]. Although the whole NETP tends to be highly stratified at the surface with an underlying StSsW, the difference between the GoT and other areas of the Mexican Pacific lies in that Tehuano events break the stratification and promote the vertical mixing and the rise of DIC-rich subsurface water (SSW), hence allowing waters with high DIC and pCO_2 concentrations reach the surface. This area showed minimum pH and Ω_{Ar} values; pH and decreased 0.6 units, while Ω_{Ar} dropped 2.6 units (68%), when compared with the surface peaks observed in the region of anticyclonic eddies. The minimum surface Ω_{Ar} (1.2) was lower than figures reported for other regions of the Eastern Tropical Pacific, such as Papagayo (~2.0–3.2) [*Rixen et al.*, 2012] and the NETP (3.3–4.1) [*Franco et al.*, 2013]. Consequently, the saturation horizon in this region of the GoT is located at only 30 m depth, thus making of it the shallowest horizon reported for the Mexican Tropical Pacific (70–100 m), similar to data reported for upwelling regions off California [*Feely et al.*, 2008; *Franco et al.*, 2014].

4.1.2 Coastal upwelling

Upwelling areas observed in the coasts of transects I and II resulted in an enrichment of DIC and pCO_2, and a drop in pH and Ω_{Ar} in surface water near the coast (section 3.2.1). The intensity of the upwelling is similar to that observed in Baja California upwelling zones [*Koračin et al.*, 2004; *Perez-Brunius et al.*, 2007], since the wind flowing parallel to the coast (~5 m s^{-1}) produces a wind stress of ~0.04 Nm^2 and an Ekman transport of 75–96 m^3 s^{-1} $100m^{-1}$. Coastal upwelling can have a significant impact not only on the coast but also at the mesoscale level, since according to *Trasviña et al.* [1995], the Tehuantepec anticyclonic eddies are fed by water from the west, i.e. the region where upwelled water is located during coastal upwelling. In their study, *Müller-Karger and Fuentes-Yaco* [2000] reported positive chlorophyll anomalies within anticyclonic eddies, which were attributed to the effect of Tehuano events. However, these anomalies may also be due to the entrance of nutrient-rich waters from upwelling events on the west coast.

Near the coast, DIC and pCO_2 values were higher than the values predicted to occur by year 2100 for the global ocean [*Hoegh-Guldberg et al.*, 2014]. Surface pH and Ω_{Ar} were similar to those reported for other upwelling regions such as Papagayo, Costa Rica (7.86–

7.92) [*Rixen et al.*, 2012], and the upwelling filament off the western African coast (pH_{Tot}=7.94–8.05) [*Loucaides et al.*, 2012]. The depth of the saturation horizon in the upwelling zone was minimal (41 m); this horizon was deeper than the one reported for Pt. St. George, California, but shallower than in the Baja California coast [*Feely et al.*, 2008]. From the above, it is clear that upwelling produces a marked variability in the CO_2 system under post-Tehuano conditions, similar to important upwelling regions elsewhere.

4.1.3 Mesoscale eddies

The key factors that determine the degree of influence of mesoscale eddies on the water column and its chemical properties are their residence time, intensity and direction of rotation [*Willett et al.*, 2006]. In the present study, the anticyclonic eddy (A1) was the largest eddy observed in Tehuantepec and the first to appear after the first Tehuano event (Figures 3–4). According to the literature this is always the case, in addition to having a longer duration than cyclonic eddies [*Clarke*, 1988; *McCreary et al.*, 1989; *Trasviña et al.*, 1995]. This means that changes in the CO_2 system are evident shortly after the wind forcing and remain over the lifetime of cyclonic eddies. Consistent with observations of *Barton et al.* [1993], this anticyclonic eddy was intensified by subsequent winds after its formation; in addition, it reached a size similar to that of other anticyclonic eddies that are typical of this area [*Palacios and Bograd*, 2005; *Willett et al.*, 2006]. Vertically, its effect in the water column is related to the sinking of isotherms down to 180 m. Although only the outer region of the eddy could be described through sampling, its center is likely deeper.

In the Gulf of Tehuantepec, the sinking of the thermocline (and, consequently, of the upper StSsW) by anticyclonic eddies contributed to surface water with minimum DIC and pCO_2 levels (pH and Ω_{Ar} maxima). This effect has been observed in other areas, such as the Haida anticyclonic eddy close to the Queen Charlotte Island, Canada, where the DIC concentration was lower within the cyclonic eddy than in the surrounding water [*Chierici et al.*, 2005]. Therefore, it is clear that low DIC concentrations lead the acid-base chemistry towards higher pH and Ω_{Ar} levels. Additionally, the accumulation of warm water promotes a stronger stratification, which further limits the exchange of DIC between subsurface and surface waters [*Franco et al.*, 2014]. As a result, the above conditions produce a mixed layer with a carbon chemistry characterized by two potential scenarios: 1) waters with DIC and pH close to equilibrium with the atmosphere, when waters are oligotrophic; or 2) waters with slightly high pH coupled with DIC below equilibrium levels, when photosynthesis processes have occurred within the eddy.

Although the limited exchange with subsurface water lowers the input of nutrients and affects primary productivity, it is possible to find positive chlorophyll anomalies in anticyclonic eddies in the GoT [*Müller-Karger and Fuentes-Yaco*, 2000]. In this case, primary production within the anticyclonic eddy might even turn it into a CO_2 sink, similar to the Haida eddy during 2001, which was reported as a CO_2 sink relative to the surrounding water [*Chierici et al.*, 2005]. Considering that Tehuantepec anticyclonic eddies have a lifetime of up to 6 months and can travel up to 2000 km to the west [*Palacios and Bograd*, 2005; *Willett et al.*, 2006], these structures may be functioning as carbon sinks with low DIC concentrations and high pH values if they contain phytoplankton biomass.

Also, this type of eddies promotes a deeper aragonite saturation horizon, hence providing a suitable habitat for calcifying organisms such as foraminifera and coccolithophores.

The Papagayo anticyclonic eddy (A2) This eddy catalyzed the disappearance of the second cyclonic eddy by increasing the dynamic height and sinking the subsurface water, which led to a drop in DIC and an increase in both pH and Ω_{Ar}. Based on numerical simulations [*Velazquez-Muñoz et al.* [2014], Papagayo eddies seem to influence circulation patterns within the GoT. However, this fact is documented for the first time through in situ data that suggest a complex interaction between the GoT and Central America. This connectivity could be an important source of exchange of chemical properties, similar to the way in which Tehuantepec cyclonic eddies export mass, heat, chemicals and organisms out of the continental shelf.

On the other hand, the cyclonic circulation covered a large part of the GoT; however, the cyclonic eddy was formed one month after the anticyclonic one, when the latter drifted away from the coast (Figure 3). The eastern eddy lasted one week and disappeared once the Papagayo eddy started approaching as it travelled westward. The fact that this type of structure requires more time to form and is weaker and ephemeral could explain why cyclonic eddies were not always detected in previous studies [*Velázquez-Muñoz et al.*, 2011]. Consequently, their physical importance and biogeochemistry have been little studied; only their relevance on primary productivity has been addressed in previous investigations [*Gonzalez-Silvera et al.* [2004].

The present study revealed that the cyclonic eddy produced shallower pycno- and thermocline, and maintained conditions that promote DIC enrichment near the surface. Surface DIC levels within the eddy exceeded those found within eddies near the Canary Islands (2095 μmol kg^{-1}) [*González-Dávila et al.*, 2006]. This is due to the Tehuantepec cyclonic eddy being deeper and the rise of isotherms being greater relative to conditions in the Canary Islands (100 m); besides, subsurface water in that region contains lower DIC concentrations (≤ 2155 μmol) compared to StSsW. In contrast, compared to the Opal eddy in Hawaii, characterized by a stronger vertical pumping (~120 m) [*Chen et al.*, 2008], our data show similar DIC concentrations in surface waters within the eddy, but higher in the rest of the water column. These differences are due to a lower DIC content in the water masses across their study region. This underlines the importance of the type of water mass and its origin in the study of both the carbon chemistry and its global balance. In our case, the pumping of DIC-rich, low-pH water (StSsW) contributes to maintain in surface water the enrichment conditions resulting from previous mixing. These dynamic and chemical conditions make of the Gulf of Tehuantepec a DIC-rich region as well as a source of carbon into the atmosphere.

The pumping of water toward the surface within cyclonic eddies increases nutrient inputs and fosters primary productivity [*Bibby et al.*, 2008; *Chen et al.*, 2008; *González-Dávila et al.*, 2006]. For the region studied here, other investigations have reported that the nutricline may be at a depth between 6 and 32 m [*Lara-Lara and Bazán-Guzmán* [2005], hence increasing productivity. However, while eddies increase nutrient levels and DIC fosters primary production, causing cyclonic eddies to function as "production islands", the shallow saturation horizon impacts $CaCO_3$ precipitation rates and might negatively affect calcifying organisms.

Based on the above discussion, the effects of mesoscale eddies on carbonate chemistry are similar to those reported for other regions of the world. The distinctive feature in the Mexican Tropical Pacific is that mesoscale eddies can account for up to 50% of the total variability of sea surface height [*Godínez et al.*, 2010] in the absence of inter-annual El Niño/La Niña conditions, and occur in a region where subsurface DIC levels are high. This fosters a greater vertical transport of DIC toward the surface when cyclonic eddies occur. In the particular case of Tehuantepec this effect could be more significant, given that mesoscale eddies are formed year-round [*Barton et al.*, 2009; *Trasviña and Barton*, 2008; *Willett et al.*, 2006]. The recurrent presence of eddies implies a constant pumping of carbon to the surface in the case of cyclonic eddies, or to deeper waters in the case of anticyclonic eddies. This highlights their importance in modulating the seasonal variability of the CO_2 system in coastal ecosystems across the region.

4.1.4 Poleward coastal current

Another mesoscale structure of importance in relation to carbon chemistry in the GoT is the coastal current that flows to the northwest. Although this has been reported previously as a surface current by other authors [*Barton et al.*, 2009; *Flores-Vidal et al.*, 2011; *Machain-Castillo et al.*, 2008; *Velázquez-Muñoz et al.*, 2011], in the present study it occurred as a surface current to the east and a subsurface one to the west. This current functions as a DIC advection mechanism. DIC concentrations are similar across all the coastal stations at the depth where this current is located, and differ from levels observed in all other stations (except for transect IV). The current runs through the mixed area and transports DIC-rich water to coastal regions located west of the study area, thereby contributing to high DIC concentrations and low pH and Ω_{Ar} levels. Therefore, this coastal current contributes to the role of this region as a source of CO_2 into the atmosphere. However, further in-depth studies are needed on this current to better understand its mechanisms and importance on the variability of the CO_2 system.

4.2 Air-sea flux of CO_2

The positive carbon flux values (FCO_2) calculated for post-Tehuano conditions indicate that the system functions as a source of CO_2 into the atmosphere. The present study reports the highest fluxes recorded to date for the Mexican Pacific, (42 mmol m^{2} d^{-1}), and the second highest for the Eastern Tropical Pacific above its oxygen-minimum zone after the upwelling in the Peruvian coasts, for which fluxes around 51 mmol C m^{-2} d^{-1} have been reported [*Friederich et al.*, 2008]. Our values are also higher than those reported for other tropical regions of Mexico (≤ 3.3 mmol m^{-2} d^{-1}, north of our study area) and the coast of Chile (0.8 - 25 mmol m^{-2} d^{-1}) [*Franco et al.*, 2014; *Paulmier et al.*, 2008].

Although CO_2 fluxes are high under post-Tehuano conditions and were observed in a small area, it is reasonable to expect that the flux of CO_2 during Tehuano conditions is even higher and comprises a greater area. Compared with other regions, the gulf of Tehuantepec contributes significantly to the carbon balance in Mexico and should be included in carbon inventories. In general, the significant CO_2 fluxes observed were due to the high carbon content in the zone mixed either by Tehuano winds or by the upwelling of surface waters associated with StSsW. In this geographic region, stratification limits carbon exchange [*Franco et al.*, 2014], while mixing produces the opposite effect, carrying DIC-enriched water toward the surface. On the other hand, the shallower the upper limit of StSsW, the greater the flux of CO_2 [*Franco et al.*, 2014]. The processes that carried this water mass closer to the surface were upwelling, followed by cyclonic eddies, both of which fostered a rise in DIC in surface water and, hence, the flux of CO_2 into the atmosphere. In contrast, anticyclonic eddies caused the sinking of this water mass, leading to CO_2 fluxes close to the equilibrium.

Observations made in the Mexican Tropical Pacific by *Franco et al.* [2014] revealed that the ocean behaves as a weak source of CO_2 (3.3 mmol m^{-2} d^{-1}) when the influence of StSsW on surface water is weak, and as a carbon sink when TSW promotes stratification. In that region, the processes regulating the influence of StSsW and DIC concentrations were advection and high stratification (~1400 J m^{-3}). As shown in Figure 8, in addition to these processes, vertical mixing, coastal upwelling and the Ekman pumping in cyclonic eddies can influence the flux of CO_2 into the atmosphere in the Gulf of Tehuantepec.

In addition to the forcing by physical processes, biological activity regulates the intensity and variability of carbon fluxes in surface water [*Wang et al.*, 2006]. This work did not estimate the effect of biological activity on the CO_2 system in the GoT. However, the extent of the biological contribution in the study area may be significant, since primary productivity increases significantly after the Tehuano forcing [*Gonzalez-Silvera et al.*, 2004]. As estimated by *Wang et al.* [2006] through a biogeochemical model coupled with oceanic circulation, primary productivity removes 0.87 Pg C per year across the equatorial Pacific, i.e. 59% of the carbon contributed by physical processes to surface water (1.47 Pg C). The April transitional period showed positive fluxes, suggesting that the GoT is a source of CO_2 into the atmosphere. Since during the post-Tehuano conditions the Gulf of Tehuantepec shows a residual flux of lesser intensity in terms of mixing and entrainment compared with the Tehuano season. In fact, if the same DIC concentrations as those reported here were considered to be under high wind conditions (20 m s^{-1}) the result would be larger. Given the maximum fluxes reported in this study (42 mmol m^{-2} d^{-1}), it can be considered that this region remains as a source of CO_2 into the atmosphere for four months approximately (~120 d), producing approximately 61 g C m^{-2}. If we consider that the Tehuano season produces a plume of cold water measuring some 400 x 200 km [*Barton et al.*, 1993], a contribution of up to 4.9 Tg C could be estimated in the plume region alone. This accounts for ~0.8% of the annual flux of CO_2 for the whole Equatorial Pacific, estimated at 0.6 Pg C [*Wang et al.*, 2006]. The increase of phytoplankton biomass after Tehuano events would also increase DIC demand, which in turn would affect FCO_2. Assuming biological DIC removal holds the same rate as in the Equatorial Pacific, primary productivity could remove as much as 2.9 Tg C, making the process more biologically-mediated, compared to conditions during a Tehuano event. However, it is important to keep in mind that the extent of such effect will depend on initial DIC concentrations, intensity of the physical forcing, redistribution by anticyclonic eddies, and time elapsed between the initial enrichment and the subsequent biological response.

4.3 Ecological implications

The increase in DIC concentrations near the surface during post-Tehuano conditions and the consequent decrease in pH and Ω_{Ar} have important implications for coastal ecosystems in the region. Low pH and Ω_{Ar} levels may be associated with negative effects on the growth, calcification rates, or survival of various species of organisms. However, the particular effects and their magnitude depend on each individual species, and also vary with the stage of the life cycle and the duration of exposure [*Price et al.*, 2011; *Tambutté et al.*, 2011]. Along with other species, the coral *Pocillopora damicornis* prospers in the GoT and is regarded as the most abundant coral species in the region [*López-Pérez et al.*, 2014]. It has been reported that pH values of 7.4 and Ω_{Ar} levels of 1.1, such as those found in this work, produce an over-regulation of genes encoding for the proteins involved in calcification, while a pH of 7.2 (RR = 0.68) decreases their regulation [*Vidal-Dupiol et al.*, 2013]. This may explain why this coral displays a higher calcification rate in regions with no upwelling events, compared with upwelling zones such as those in Panama and the Galápagos Islands [*Manzello*, 2010]. The calcification rate of *Pocillopora meandrina* has been observed to decrease by 50% when exposed to water with an aragonite saturation state of 2.0 [*Muehllehner and Edmunds*, 2008]. In this investigation, more than 50% of the stations studied (19 out of 26) showed Ω_{Ar} values lower than 2.0 in the first 30 m. In the present investigation, pH and Ω_{Ar} values of 7.7 and 1.4, respectively, were recorded in the center of the cyclonic eddy at depths less than 27 m (Figure 9a and b). Similar values (pH=7.7, Ω_{Ar}=) were recorded at 10 m depth, at the station nearest to the coastline, 6 km off Puerto Angel, Oax. Although there are no records about the variability of the carbonate system on the coral reefs inside the GoT, temperature data from *Glynn and Morales* [1997] suggest Tehuano events have a direct effect on the coastal oceanography of the region, and therefore corals are being exposed to DIC-rich water with StSsW content. *Glynn and Morales* [1997] registered a 4°C decrease in seawater temperature (from ~24 to ~20°C) at the reef base (8 m depth) in La Entrega coral reef, Huatulco,Oaxaca, during a six-day survey on February 1996, right after two Tehuano events of 17 and 15 m s^{-1} took place in the GOT (February 12-14 and 17), as registered on Seawinds satellite data [*Zhang et al.*, 2006b]. According to *Barton et al.* [2009], who carried out an oceanographic sampling campaign at the GoT around the same time (February 10-27, 1996), the cold water plume was located near the coast of Huatulco, where surface temperatures were 25°C. These autors observed that the cold water plume produced in the central GoT is generally displaced westward during wind relaxation and therefore may approach the coast of Huatulco. The vertical distribution of water properties near Huatulco showed the ascencion of StSsW near the coast as a response to wind-forcing. Based on our findings, it is considered that these and similar species are being exposed to water with Ω_{Ar} that is suboptimal for their development. Further coastal records regarding pH and Ω_{Ar} variability are needed to confirm this finding.

According to *López-Pérez et al.* [2014], only 14 of the 34 coral species living in the Mexican Pacific [*Reyes-Bonilla et al.*, 2010] are distributed along the coast of Oaxaca. Furthermore, *López-Pérez and Hernández-Ballesteros* [2004] report that coral populations in Huatulco, Oaxaca, are a mixture of patches under various recovery stages. Preliminary results from an ongoing investigation indicate that, among the coral species living in the area, *Porites panamensis* displays the lowest growth, density, and calcification rates in the Mexican Pacific. These figures are 50% lower in our study area [A. Lopez-Perez, unpublished data, 2015] than the minimum values registered in Marietas Islands in the central region of the Mexican Pacific where the StSsW is also present, albeit with a lesser contact with the surface [*Franco et al.*, 2014; *Norzagaray-López et al.*, 2013]. In turn, corals of *P. panamensis* living in the Marietas Islands region display lower growth and calcification rates relative to those in Baja California. In Puerto Angel, Oaxaca, this species is extremely rare and prospers only in the upper three meters of depth [*Norzagaray-López et al.*, 2013; *Reyes-Bonilla and Leyte-Morales*, 1998]. The low pH and Ω_{Ar} may be negatively affecting the abundance, distribution, and calcification rate of corals. However, the coastal zone displays high variability and is also influenced by other processes (river inputs, eutrophication, waves, etc.) that modulate the degree of exposure of corals to corrosive water.

Other calcifying organisms in the GoT, such as foraminifera and coccolitophores, may also be exposed to low pH values. According to *Machain-Castillo et al.* [2008], shells of recent planktonic foraminifera in GoT sediments show differences in assemblages, depeding on the location of the wind jet, with *Globigerina bulloides* being the most abundant species (21%). Shell dissolution rates were higher near the coast (15.5 - 16.5 N and 95 - 95.5 W), at the same location of the highly mixed area in our study. Nitrate concentations in the overlying water column (21 μM at 50 m depth) confirmed the influence of subsurface water (1 - 21 μM). However, foraminifera showed a wide range of inter- and intra-specific responses to [CO_3^{-2}] variability [*Aldridge et al.*, 2012], as their calcification intensity and dissolution rate respond to different environmental drivers and calcification strategies [*de Nooijer et al.*, 2009]. Previous studies indicate that along with [CO_3^{-2}] availabilty, ortophosphate levels also affect calcification and promote dissolution.

The relative contribution of the different environmental drivers is unknown for most foraminifera species. *Globigerina bulloides* from the North Atlantic Ocean showed a positive correlation between size-normalized weight (SNW, an indicator of calcification in foraminifera) and $[CO_3^{-2}]$, but the negative correlation of SNW with ortophospate and nitrate was higher [*Aldridge et al.*, 2012]. Benthic foraminifera from hydrothermal vents in the Gulf of Baja California and Ischia Island, Italy, showed shifts and impoverishment of assemblages, as well as an increased post-mortem dissolution at pH values of 7.5 - 7.8, which supassed the minima found in our study [*Dias et al.*, 2010; *Pettit et al.*, 2013]. These changes may affect foraminifera in the long term, as reported by Moy et al. [2009], who found that modern shells of *G. bulloides* are 30–35% lighter than those from the Holocene. Coccolitophorides display a similar response, with some species being more suceptible to test dissolution than others. According to *Müller et al.* [2010], *Emiliana huxlei* and *Coccolithus braarudii* displayed a 9% and 29% drop in growth rate, respectively, when exposed to water with pCO_2 values of 1150 and 930 μatm, respectively. In our study such pCO_2 values were observed near the coast at the first 30 m depth. In addition, some species of both foraminifera and coccolitophorids have developed metabolic strategies to cope with variations in pH and $[CO_{3\text{-}2}]$ [*de Nooijer et al.*, 2009; *Taylor et al.*, 2011], *i.e.* increasing cell pH to favor the formation and precipitation of $[CO_3^{-2}]$ at the expense of other metabolic functions. Therefore, we would expect these calcifying groups to be affected by the variability of the carbon system inside the GoT; however, exposure studies with local species are needed to confirm and quantify this effect.

The presence of coral reefs and other calcifiers in the region raises several questions: how do they survive in such conditions? Is exposure to water sufficiently extensive/intense to cause negative effects? Have organisms living in the GoT developed adaptative strategies to withstand these conditions? If they have indeed adapted, this region could serve as a window into the future under an ocean acidification scenario, since many of the pH values reported here are lower than those predicted to occur in tropical regions by year 2100 (7.7). Furthermore, the GoT may act as a positive feedback to climate change; according to *Ishii et al.* [2014], half of the carbon that enters the Pacific ocean in the extratropics is released back to the atmosphere at the tropics. This implies that under a climate change scenario, the increase in anthropogenic carbon would result in a larger DIC enrichement of the StSsW. On the other hand, the rising sea surface temperature decreases CO_2 solubility and enhances stratification of the water column, mantaining DIC-rich conditions under the thermocline, until Tehuano events disrupt the water column and promote DIC to surface and return to the atmosphere, increasing FCO_2. These conditions will further decrease pH and Ω_{Ar}. However, as the water column is already enriched with DIC, the change rate may be lower than in temperate regions. To understand these processes, further studies are needed, focusing on the variability of the carbonate system in the GoT at different spatial and temporal scales, as well as studies on the exposure of various GoT native organisms to these conditions, in order to deepen our understanding of how pH and Ω_{Ar} influence coral reef-building species and other calcifying organisms that inhabit Gulf of Tehuantepec coastal ecosystems.

5 Conclusions

This investigation analyzed the post-Tehuano oceanographic conditions in the Gulf of Tehuantepec and their effect on the CO_2 system. The main oceanographic structures observed were areas of high mixing near the head of the gulf, areas with coastal upwelling, mesoscale eddies, and a coastal current flowing to the west; all of these co-occurred during April 2013. This complex set of structures produced significant changes in the chemistry of dissolved inorganic carbon (DIC). The highly mixed region showed the highest surface DIC concentrations and pCO_2 values, high air-sea CO_2 fluxes, and minimum surface pH and aragonite saturation levels. These values exceed those predicted for the global ocean in year 2100, and are among the most extreme conditions reported for the Mexican Pacific. Coastal upwelling and the cyclonic eddy led to the lifting of isolines of high DIC concentration (low pH and Ω_{Ar}) corresponding to StSsW close to the surface. By contrast, anticyclonic eddies caused the sinking of the StSsW, which is the main source of DIC in the region. The coastal current transported water toward the west, redistributing previously mixed water; this led to the advection of DIC to the west of the study area.

The estimated carbon fluxes are the highest reported for the Mexican Pacific and rank second across the Tropical Eastern Pacific, even when determined under post-Tehuano conditions. The findings reported in this paper suggest that the study region is a major source of CO_2 into the atmosphere and should be included in carbon inventories. Our results highlight the importance of regions whose dynamics is dominated by winds jets in the global carbon balance.

6 Acknowledgments

We thank two anonimous reviewers for their valuable comments and suggestions, which improved the manusctipt. The AVHRR Oceans Pathfinder project of the NASA Jet Propulsion Laboratory and Physical Oceanography Distributed Active Archive Center provided satellite wind data. The data of anomaly in the sea level are produced by Segment Sun Altimetrie et Orbitographie/Developing Use of Altimetry for Climate Studies (Ssalto/Duacs) and distributed by Archiving Validation and interpretation of satellite Oceanographic Data (Warning), with the support of the Center National d'Etudes Spatiales (CNES). The National Council for Science and Technology (CONACyT) provided financial support for the first author (grant 266585). Part of the sampling materials was funded by project UMAR-2IR0906 "System of carbonates in the Gulf of Tehuantepec". The participation of EB is part of the Project ¨A study of the Mexican Coastal Current and the adjacent Pacific, with a SeaGlider, oceanographic cruises and satellite data¨ supported by CONACyT (SEP-2011rucerosxica). We are grateful to the Secretaría de Marina and its Salina Cruz Oceanographic Research Station for access to cruise ships and CTD data; in particular, to Cap. José Paul Murad Serrano, Cap. CG DEM José Luis Eguileta Arias and the RV Altair crew. María Elena Sánchez Salazar translated the manuscript into English and also assisted in the editorial review. This is PMEL contribution #4382. Access the data used write to jmartin@uabc.edu.mx.

7 References

Adams, D. K., and G. R. Flierl (2010), Modeled interactions of mesoscale eddies with the East Pacific Rise: Implications for larval dispersal, *Deep Sea Research Part I: Oceanographic Research Papers*, *57*(10), 1163-1176.

Aldridge, D., C. Beer, and D. Purdie (2012), Calcification in the planktonic foraminifera Globigerina bulloides linked to phosphate concentrations in surface waters of the North Atlantic Ocean, *Biogeosciences*, *9*(5), 1725-1739.

Barton, E. D., M. F. Lavín, and A. Trasviña (2009), Coastal circulation and hydrography in the Gulf of Tehuantepec, Mexico, during winter, *Continental Shelf Research*, *29*(2), 485-500.

Barton, E. D., M. L. Argote, J. Brown, M. Kosro, M. F. Lavin, J. M. Robles, and R. L. Smith (1993), Supersquirt: Dynamics of the Gulf of Tehuantepec Mexico, *Oceanography*, *6*(1), 23-30.

Bibby, T. S., M. Y. Gorbunov, K. W. Wyman, and P. G. Falkowski (2008), Photosynthetic community responses to upwelling in mesoscale eddies in the subtropical North Atlantic and Pacific Oceans, *Deep Sea Research Part II: Topical Studies in Oceanography*, *55*(10–13), 1310-1320.

Cepeda-Morales, J., G. Gaxiola-Castro, E. Beier, and V. M. Godínez (2013), The mechanisms involved in defining the northern boundary of the shallow oxygen minimum zone in the eastern tropical Pacific Ocean off Mexico, *Deep-Sea Research Part I*, *76*, 1-12.

Clarke, A. J. (1988), Inertial wind path and sea surface temperature patterns near the Gulf of Tehuantepec and Gulf of Papagayo, *Journal of Geophysical Research: Oceans*, *93*(C12), 15491-15501.

Chang, C. H., S. P. Xie, N. Schneider, B. Qiu, J. Small, W. Zhuang, B. Taguchi, H. Sasaki, and X. Lin (2012), East Pacific ocean eddies and their relationship to subseasonal variability in Central American wind jets, *Journal of Geophysical Research: Oceans (1978–2012)*, *117*(C10).

Chen, F., W.-J. Cai, C. Benitez-Nelson, and Y. Wang (2007), Sea surface pCO_2-SST relationships across a cold-core cyclonic eddy: Implications for understanding regional variability and air-sea gas exchange, *Geophys. Res. Lett.*, *34*(10), L10603.

Chen, F., W.-J. Cai, Y. Wang, Y. M. Rii, R. R. Bidigare, and C. R. Benitez-Nelson (2008), The carbon dioxide system and net community production within a cyclonic eddy in the lee of Hawaii, *Deep Sea Research Part II: Topical Studies in Oceanography*, *55*(10), 1412-1425.

Chierici, M., L. A. Miller, F. A. Whitney, K. W. Johnson, and C. S. Wong (2005), Biogeochemical evolution of the carbon dioxide system in the waters of long-lived mesoscale eddies in the Northeast Pacific Ocean, *Deep Sea Research Part II: Topical Studies in Oceanography*, *52*(7–8), 955-974.

de Nooijer, L. J., T. Toyofuku, and H. Kitazato (2009), Foraminifera promote calcification by elevating their intracellular pH, *Proceedings of the National Academy of Sciences*, *106*(36), 15374-15378.

Dias, B., M. Hart, C. Smart, and J. Hall-Spencer (2010), Modern seawater acidification: the response of foraminifera to high-CO2 conditions in the Mediterranean Sea, *Journal of the Geological Society*, *167*(5), 843-846.

Feely, R. A., R. Wanninkhof, C. Goyet, D. E. Archer, and T. Takahashi (1997), Variability of CO_2 distributions and sea-air fluxes in the central and eastern equatorial Pacific during the 1991–1994 El Niño, *Deep Sea Research Part II: Topical Studies in Oceanography*, *44*(9–10), 1851-1867.

Feely, R. A., C. L. Sabine, J. M. Hernandez-Ayon, D. Ianson, and B. Hales (2008), Evidence for Upwelling of Corrosive "Acidified" Water onto the Continental Shelf, *Science*, *320*, 1490-1492.

Fiedler, P. C. (1992), Seasonal Climatologies and variability of Eastern Tropical Pacific Suface Waters., *U.S. Departamente of Commerce*.

Fiedler, P. C., and L. D. Talley (2006), Hydrography of the eastern tropical Pacific: A review, *Progress In Oceanography*, *69*(2–4), 143-180.

Fiedler, P. C., R. Mendelssohn, D. M. Palacios, and S. J. Bograd (2013), Pycnocline Variations in the Eastern Tropical and North Pacific, 1958–2008, *Journal of Climate*, *26*(2), 583-599.

Flores-Vidal, X., R. Durazo, C. Chavarme, and P. Flament (2011), Circulación costera en ausencia de viento en el golfo de Tehuantepec, México: Observaciones con radares de alta frecuencia, *Ciencias Marinas*, *37*, 493-512.

Flores-Vidal, X., R. Durazo, L. Zavala-Sansón, P. Flament, C. Chavanne, F. J. Ocampo-Torres, and C. Reyes-Hernández (2014), Evidence of inertially generated coastal-trapped waves in the eastern tropical Pacific, *Journal of Geophysical Research: Oceans*, *119*(5), 3121-3133.

Franco, A. C. (2011), Flujo de carbono y subsaturación de carbonato en la zona de mínimo de oxígeno del Pacífico Tropical Mexicano, 116 pp, Universidad Autónoma de Baja California.

Franco, A. C., M. Hernández-Ayón, E. Beier, H. Maske, A. Olivos-Ortíz, R. Sosa-Ávalos, R. Roa-Mendoza, A. Siqueiros-Valencia, and J. Farber (2013), Subsaturación de carbonato en la zona de mínimo de oxígeno (ZMO) de las costas del Pacífico Tropical frente a México, in *Estado Actual del Conocimiento del Ciclo del Carbono y sus Interacciones en México: Síntesis a 2013*, edited by Fernando Paz Pellat, Julio Wong González, M. Bazan and V. Saynes, pp. 414-420, Programa Mexicano del Carbono, México, D.F.

Franco, A. C., J. M. Hernández-Ayón, E. Beier, V. Garçon, H. Maske, A. Paulmier, J. Färber-Lorda, R. Castro, and R. Sosa-Ávalos (2014), Air-sea CO2 fluxes above the stratified oxygen minimum zone in the coastal region off Mexico, *Journal of Geophysical Research: Oceans*, n/a-n/a.

Friederich, G. E., J. Ledesma, O. Ulloa, and F. P. Chavez (2008), Air–sea carbon dioxide fluxes in the coastal southeastern tropical Pacific, *Progress In Oceanography*, *79*(2), 156-166.

Glynn, P., and G. L. Morales (1997), Coral reefs of Huatulco, West Mexico: reef development in upwelling Gulf of Tehuantepec, *Revista de Biología Tropical*, *45*(3), 1033-1047.

Godínez, V. M., E. Beier, M. F. Lavín, and J. A. Kurczyn (2010), Circulation at the entrance of the Gulf of California from satellite altimeter and hydrographic observations, *Journal of Geophysical Research*, *115*(C4).

González-Dávila, M., J. M. Santana-Casiano, D. de Armas, J. Escánez, and M. Suarez-Tangil (2006), The influence of island generated eddies on the carbon dioxide system, south of the Canary Islands, *Marine Chemistry*, *99*(1), 177-190.

Gonzalez-Silvera, A., E. Santamaria-del-Angel, R. Millán-Nuñez, and H. Manzo-Monroy (2004), Satellite observations of mesoscale eddies in the Gulfs of Tehuantepec and

Papagayo (Eastern Tropical Pacific), *Deep Sea Research Part II: Topical Studies in Oceanography*, *51*(6-9), 587-600.

Hernandez-Ayon, J. M., C. Chapa-Balcorta, F. Delgadillo-Hinojosa, V. F. Camacho-Ibar, M. A. Huerta-Díaz, E. Santamaría-del-Angel, S. Galindo-Bect, and J. A. Segovia-Zavala (2013), Dynamics of dissolved inorganic carbon in the Midriff Islands region of the Gulf of California: Influence of water masses Dinámica del carbono inorgánico disuelto en la región de las grandes islas del golfo de California: Influencia de las masas de agua, *Ciencias Marinas*, *39*(2), 183-201.

Hoegh-Guldberg, O., R. Cai, E. S. Poloczanska, P. G. Brewer, S. Sundby, K. Hilmi, V. J. Fabry, and S. Jung (2014), The Ocean, in *Climate Change 2014: Impacts, Adaptation, and Vulnerability. Part B: Regional Aspects. Contribution of Working Group II to the Fifth Assessment Report of the Intergovernmental Panel on Climate Change*, edited by V. R. Barros, et al., pp. 1655-1731, Cambridge University Press, Cambridge, United Kingdom and New York, NY, USA.

Ishii, M., R. Feely, K. Rodgers, G.-H. Park, R. Wanninkhof, D. Sasano, H. Sugimoto, C. Cosca, S. Nakaoka, and M. Telszewski (2014), Air–sea CO_2 flux in the Pacific Ocean for the period 1990–2009, *Biogeosciences*, *11*(3), 709-734.

Johnson, K., J. Sieburth, P. Williams, and L. Brändström (1987), Coulometric total carbon dioxide analysis for marine studies: Automation and calibration, *Marine Chemistry*, *21*(2), 117-133.

Koračin, D., C. E. Dorman, and E. P. Dever (2004), Coastal Perturbations of Marine-Layer Winds, Wind Stress, and Wind Stress Curl along California and Baja California in June 1999, *Journal of physical oceanography*, *34*(5), 1152-1173.

Lara-Lara, J. R., and C. Bazán-Guzmán (2005), Distribución de clorofila y producción primaria por clases de tamaño en la costa del Pacífico mexicano. Distribution of chlorophyll and primary production by size classes along the Mexican Pacific coast, *Ciencias Marinas*, *31*(1A), 11-21.

Large, W. G., and S. Pond (1981), Open Ocean Momentum Flux Measurements in Moderate to Strong Winds, *Journal of physical oceanography*, *11*(3), 324-336.

Lewis, E., and D. W. R. Wallace (1998), Program Developed for CO_2 System Calculations, edited by ORNL/CDIAC-105a., Carbon Dioxide Information Analysis Center, Oak Ridge National Laboratory, U.S. Department of Energy, Oak Ridge, Tennessee. .

López-Pérez, A., R. Granja-Fernández, C. Aparicio-Cid, R. C. Zepeta-Vilchis, A. M. Torres-Huerta, F. Benítez-Villalobos, D. A. López-López, C. Cruz-Antonio, and O. Valencia-Méndez (2014), Corales pétreos, equinodermos y peces asociados a comunidades y arrecifes coralinos del Parque Nacional Huatulco, Pacífico sur mexicano, *Revista Mexicana de Biodiversidad*, *85*(4), 1145-1159.

López-Pérez, R. A., and L. M. Hernández-Ballesteros (2004), Coral community structure and dynamics in the Huatulco area, western Mexico, *Bulletin of Marine Science*, *75*(3), 453-472.

Loucaides, S., T. Tyrrell, E. P. Achterberg, R. Torres, P. D. Nightingale, V. Kitidis, P. Serret, M. Woodward, and C. Robinson (2012), Biological and physical forcing of carbonate chemistry in an upwelling filament off northwest Africa: Results from a Lagrangian study, *Global Biogeochemical Cycles*, *26*(3), GB3008.

Lueker, T. J., A. G. Dickson, and C. D. Keeling (2000), Ocean pCO2 calculated from dissolved inorganic carbon, alkalinity, and equations for K1 and K2: validation based on laboratory measurements of CO2 in gas and seawater at equilibrium, *Marine Chemistry*, *70*(1–3), 105-119.

Machain-Castillo, M. L., M. A. Monreal-Gómez, E. Arellano-Torres, M. Merino-Ibarra, and G. González-Chávez (2008), Recent planktonic foraminiferal distribution patterns and their relation to hydrographic conditions of the Gulf of Tehuantepec, Mexican Pacific, *Marine Micropaleontology*, *66*(2), 103-119.

Manzello, D. (2010), Coral growth with thermal stress and ocean acidification: lessons from the eastern tropical Pacific, *Coral Reefs*, *29*(3), 749-758.

McCreary, J. P., H. S. Lee, and D. B. Enfield (1989), The response of the coastal ocean to strong offshore winds: With application to circulations in the Gulfs of Tehuantepec and Papagayo, *Journal of Marine Research*, *47*(1), 81-109.

Moy, A. D., W. R. Howard, S. G. Bray, and T. W. Trull (2009), Reduced calcification in modern Southern Ocean planktonic foraminifera, *Nature Geosci*, *2*(4), 276-280.

Muehllehner, N., and P. Edmunds (2008), Effects of ocean acidification and increased temperature on skeletal growth of two scleractinian corals, Pocillopora meandrina and Porites rus, paper presented at Proceedings of the 11th International Coral Reef Symposium, Ft. Lauderdale, Florida.

Müller-Karger, F. E., and C. Fuentes-Yaco (2000), Characteristics of wind-generated rings in the eastern tropical Pacific Ocean, *Journal of Geophysical Research*, *105*(C1), 1271-1284.

Müller, M. N., K. G. Schulz, and U. Riebesell (2010), Effects of long-term high CO2 exposure on two species of coccolithophores, *Biogeosciences*, *7*, 1109–1116.

Norzagaray-López, O., M. d. C. Ávila-López, C. Chapa-Balcorta, L. Calderón-Aguilera, and M. Hernández-Ayón (2013), Reducida producción de CaCO3 por Porites panamensis en tres comunidades arrecifales del Pacífico mexicano, in *Estado Actual del Conocimiento del Ciclo del Carbono y sus Interacciones en México: Síntesis a 2013*, edited by Fernando

Paz Pellat, Julio Wong González, M. Bazan and V. Saynes, pp. 437-441, Programa Mexicano del Carbono, México, D.F.

O'Connor, B. M., R. A. Fine, K. A. Maillet, and D. B. Olson (2002), Formation rates of subtropical underwater in the Pacific Ocean, *Deep Sea Research Part I: Oceanographic Research Papers*, *49*(9), 1571-1590.

Palacios, D. M., and S. J. Bograd (2005), A census of Tehuantepec and Papagayo eddies in the northeastern tropical Pacific, *Geophysical Research Letters*, *32*(23), L23606.

Paulmier, A., D. Ruiz-Pino, and V. Garçon (2008), The oxygen minimum zone (OMZ) off Chile as intense source of CO_2 and N_2O, *Continental Shelf Research*, *28*(20), 2746-2756.

Perez-Brunius, P., M. Lopez, A. Pares-Sierra, and J. Pineda (2007), Comparison of upwelling indices off Baja California derived from three different wind data sources*Rep.*, 204-214 pp.

Pettit, L. R., M. B. Hart, A. N. Medina-Sánchez, C. W. Smart, R. Rodolfo-Metalpa, J. M. Hall-Spencer, and R. M. Prol-Ledesma (2013), Benthic foraminifera show some resilience to ocean acidification in the northern Gulf of California, Mexico, *Marine Pollution Bulletin*, *73*(2), 452-462.

Price, N., S. Hamilton, J. Tootell, and J. Smith (2011), Species-specific consequences of ocean acidification for the calcareous tropical green algae Halimeda, *Marine Ecology Progress Series*, *440*, 67-78.

Reyes-Bonilla, H., and G. E. Leyte-Morales (1998), Corals and coral reefs of the Puerto Angel region, west coast of México, *Revista de Biología Tropical*, *46*(3), 679-681.

Reyes-Bonilla, H., L. E. Calderón-Aguilera, G. Cruz-Piñón, R. A. López-Pérez, and P. Medina-Rosas (2010), Evaluación de la diversidad gama de corales arrecifales (Scleractinia) en el Pacífico de México, *Revista Mexicana de Biodiversidad*, 113-121.

Rixen, T., C. Jiménezz, and J. Cortés (2012), Impact of upwelling events on the seawater carbonate chemistry and dissolved oxygen concentration in the Gulf of Papagayo (Culebra Bay), Costa Rica: Implications for coral reefs., *Revista de Biología Tropical*, *60*(2), 187-195.

Romero-Centeno, R., J. Zavala-Hidalgo, and G. B. Raga (2007), Midsummer Gap Winds and Low-Level Circulation over the Eastern Tropical Pacific, *Journal of Climate*, *20*, 3768-3784.

Samuelsen, A., and J. J. O'Brien (2008), Wind-induced cross-shelf flux of water masses and organic matter at the Gulf of Tehuantepec, *Deep Sea Research Part I: Oceanographic Research Papers*, *55*(3), 221-246.

Schwing, F. B., M. O'Farrell, J. M. Steger, and K. Baltz (1996), Coastal Upwelling indices, west coast of North America 1946-95*Rep.*, Pacific Grove, California 93950-2097.

Simpson, J., and D. Bowers (1981), Models of stratification and frontal movement in shelf seas, *Deep Sea Research Part A. Oceanographic Research Papers*, *28*(7), 727-738.

Tambutté, S., M. Holcomb, C. Ferrier-Pagès, S. Reynaud, É. Tambutté, D. Zoccola, and D. Allemand (2011), Coral biomineralization: From the gene to the environment, *Journal of Experimental Marine Biology and Ecology*, *408*(1–2), 58-78.

Taylor, A. R., A. Chrachri, G. Wheeler, H. Goddard, and C. Brownlee (2011), A Voltage-Gated H⁺ Channel Underlying pH Homeostasis in Calcifying Coccolithophores, *PLoS Biol*, *9*(6), e1001085.

Trasviña, A., and E. D. Barton (2008), Summer circulation in the Mexican tropical Pacific, *Deep Sea Research Part I: Oceanographic Research Papers*, *55*(5), 587-607.

Trasviña, A., E. D. Barton, J. Brown, H. S. Velez, P. M. Kosro, and R. L. Smith (1995), Offshore wind forcing in the Gulf of Tehuantepec, Mexico: The asymmetric circulation, *Journal of Geophysical Research*, *100*(C10), 20,649-620,663.

Van Heuven, S., D. Pierrot, E. Lewis, and D. Wallace (2009), MATLAB Program developed for CO2 system calculations, *Rep. ORNL/CDIAC-105b*.

Velazquez-Muñoz, F. A., J. A. Martínez, and R. Durazo (2014), Numerical Simulation of Ocean Response by Offshore Wind Stress Events, in *Experimental and Computational Fluid Mechanics*, edited by J. Klapp and A. Medina, pp. 93-110, Springer International Publishing.

Velázquez-Muñoz, F. A., J. A. Martínez, C. Chavanne, R. Durazo, and P. Flament (2011), Wind-driven coastal circulation in the Gulf of Tehuantepec, Mexico, *Ciencias Marinas*, *37*(4A), 443-456.

Vidal-Dupiol, J., D. Zoccola, E. Tambutté, C. Grunau, C. Cosseau, K. M. Smith, M. Freitag, N. M. Dheilly, D. Allemand, and S. Tambutté (2013), Genes Related to Ion-Transport and Energy Production Are Upregulated in Response to CO2-Driven pH Decrease in Corals: New Insights from Transcriptome Analysis, *PLoS ONE*, *8*(3), e58652.

Wang, X., J. R. Christian, R. Murtugudde, and A. J. Busalacchi (2006), Spatial and temporal variability of the surface water pCO2 and air-sea CO2 flux in the equatorial Pacific during 1980–2003: A basin-scale carbon cycle model, *Journal of Geophysical Research: Oceans*, *111*(C7), C07S04.

Wanninkhof, R. (1992), Relationship Between Wind Speed and Gas Exchange Over the Ocean, *Journal of Geophysical Research*, *97*(C5), 7373-7382.

Weiss, R. F. (1974), Carbon dioxide in water and seawater: the solubility of a non-ideal gas, *Marine Chemistry*, *2*(3), 203-215.

Willett, C. S., R. R. Leben, and M. F. Lavín (2006), Eddies and Tropical Instability Waves in the eastern tropical Pacific: A review, *Progress In Oceanography*, *69*(2-4), 218-238.

Wyrtki, K. (1967), Circulation and water masses in the Eastern Equatorial Pacific Ocean *International Journal of Oceanology and Limnology*, *1*(2), 117-147.

Zhang, H.-M., R. W. Reynolds, and J. J. Bates (2006a), Blended and Gridded High Resolution Global Sea Surface Wind Speed and Climatology from Multiple Satellites: 1987 - Present, in *American Meteorological Society 2006 Annual Meeting,*, edited, Atlanta, GA, USA.

Zhang, H. M., J. J. Bates, and R. W. Reynolds (2006b), Assessment of composite global sampling: Sea surface wind speed, *Geophysical Research Letters*, *33*(17).

FIGURE LIST

Figure 1. Study area. Blue symbols represent the sampling grid in the Gulf of Tehuantepec. Oceanographic sections are indicated in Roman numbers I to V.

Figure 2. T-S diagrams for the cruise carried out April 13-18, 2013. (a) All T-S data. Dark red color indicates data of 200 dbar and over. (b) Selected profiles located at the mesoscale eddies, for the anticyclonic eddy (red) cyclonic eddy (blue), and the area most affected by the wind adjacent to the coast (magenta). (c) T-S-DIC plot for discrete samples (0-200 m of depth). TSW: Tropical Surface Water. StSsW: Subtropical Subsurface Water.

Figure 3.Wind conditions previous and during the sampling campaign. a) Wind velocity (m s^{-1}) from March 1 to April 19’ 2013 at 15.5°N and 95°W. The green shaded area indicates the sampling period. b) Mean wind stress (N m^{-2}) during Tehuano winds between March 1 and April 11, 2013. c) Mean post-Tehuano wind stress (N m^{-2}) between April 12 and 18, 2013. Note the different color scales used for strong and weak winds.

Figure 4. Vertical distribution of properties within the upper 200 m for sections I-V. (a) Line contours are σ_θ (kg m^{-3}) while colors indicate temperature (°C). Black triangles in (a) specify the location of CTD casts. (b) Geostrophic velocity (m s^{-1}) relative to 300 dbar. Positive velocities represent poleward (westward) currents, (c) dissolved inorganic carbon (µmol kg^{-1}), (d) *in situ* $pH_{sw,}$ (e) Ω_{Ar} and (f) pCO_2 (µatm). The aragonite saturation horizon (Ω_{Ar}=1) is shown as a black contour. The red, green, blue and purple bars at the top of the figure indicate the stations most influenced by anticyclonic eddies, coastal upwelling, cyclonic eddies, and vertical mixing, respectively.

Figure 5. Altimetry Sea surface height anomaly (cm) and associated geostrophic currents (m s^{-1}), showing the evolution of eddies at the Gulf of Tehuantepec and its vicinity, Previous to Tehuano events (March 1), right after the four Tehuano events (March 29) and during the sampling campaign (April 13-19, 2013). C1= Tehuantepec cyclonic eddy. A1=Tehuantepec anticyclonic eddy. A2= Papagayo anticyclonic eddy. The sampling cruise grid is shown in magenta in April 13 and 18 panel. (http://www.aviso.oceanobs.com/duacs/).

Figure 6. Distribution of water sample measurements obtained during April, 2013 at surface (left) and 20 m deep (right). σ_θ (kg m^{-3}) (a, d), (b, e) dissolved inorganic carbon (µmol kg^{-1}), and (c, f) *in situ* pH_{sw}. C1= cyclonic eddy. A1= anticyclonic eddy. A2= anticyclonic flow. Arrows indicate eddy location.

Figure 7. Air-Sea CO_2 flux (mmol C m^{-2} d^{-1}) in the Gulf of Tehuantepec during April 13-18, 2013. The white contour indicates the flux threshold of zero mmol C m^{-2} d^{-1}. Positive values indicate fluxes toward the atmosphere.

Figure 8. Processes involved in the variability of the CO_2 system at the Gulf of Tehuantepec during Post-Tehuano conditions. Red and blue colors indicate CO_2 sources and sinks and respectively.

Figure 9. Coverage of water with inorganic carbon chemistry attributes below the optimum for coral calcifiers. Zonal variation of a) DIC concentration, b) pH, and c) Ω_{Ar} values at the outermost stations. The x axis describes distance from west to east. d) Depth of the 2200 µmol kg^{-1} DIC contour line and e) that of $\Omega_{Ar} \leq 1.4$, f) Location of the stations shown in (a) to (c).

Table 1. Surface and subsurface water masses identified at the study area and their chemical properties.

	Water mass	
	Tropical Surface Water (TSW)	Subtropical Subsurface Water (StSsW)
Temperature	T >25°C	9≤T≤18°C
Salinity	S<34.9, Higher salinity values during Mar-May.	34.5≤S≤35.0
Geographic range	5°N - 15°N, Isotherm 25	From South Pacific to 23°N
Vertical range	0~50 m.	70-500 m
Origin	Eastern Tropical Pacific	South Pacific gyre
DIC concentration	1906±29 µmol kg^{-1}	2252-2268 µmol kg^{-1}
pCO_2	560±260 µatm	1290-1340 µatm
Dissolved Oxygen	>150 µmol kg^{-1}	<30
References	[*Cepeda-Morales et al.*, 2013; *Fiedler*, 1992; *Fiedler and Talley*, 2006; *Franco et al.*, 2014; *Wyrtki*, 1967]iedler y Talley, 2006; Cepeda-Morales *et al.*, 2013; Franco *et al.*, 2014)	[*Cepeda-Morales et al.*, 2013; *Franco*, 2011; *O'Connor et al.*, 2002]

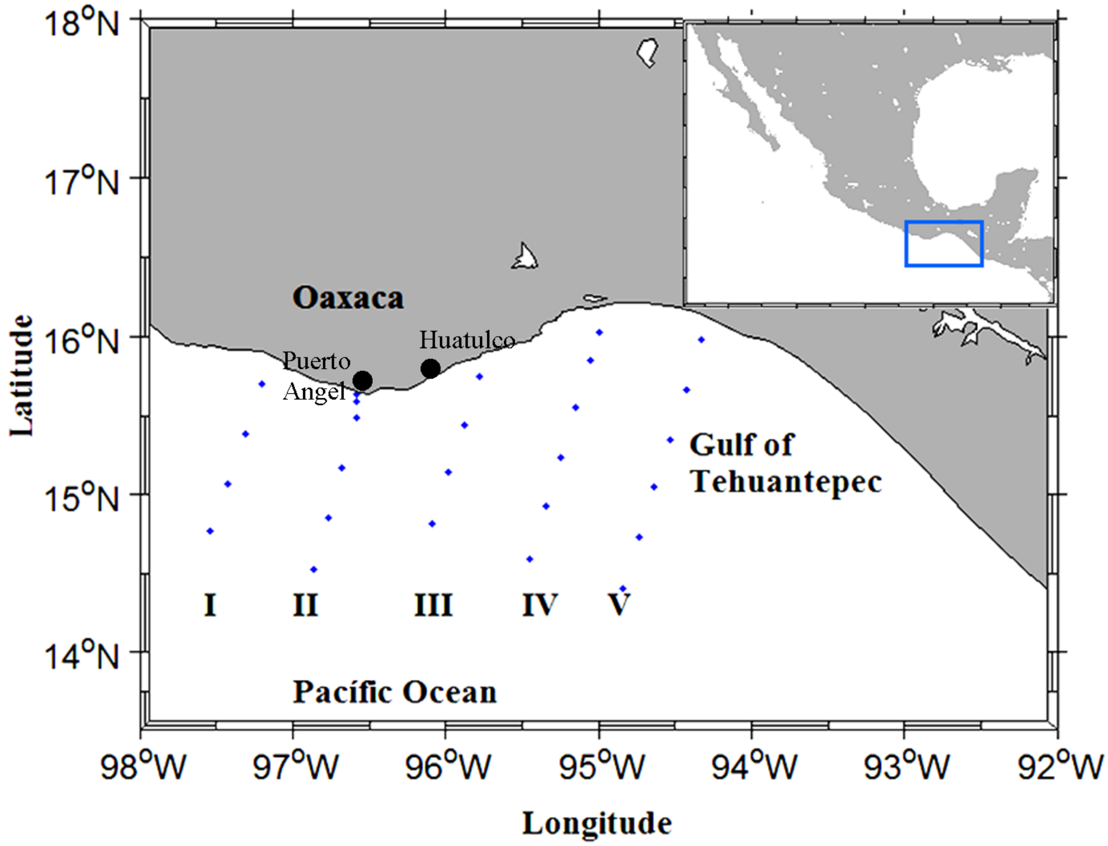
18°N
17°N
16°N
15°N
14°N
Latitude
98°W
97°W
96°W
95°W
94°W
93°W
92°W
Longitude
Oaxaca
Huatulco
Puerto
Angel
Gulf of
Tehuantepec
I
II
III
IV
V
Pacific Ocean

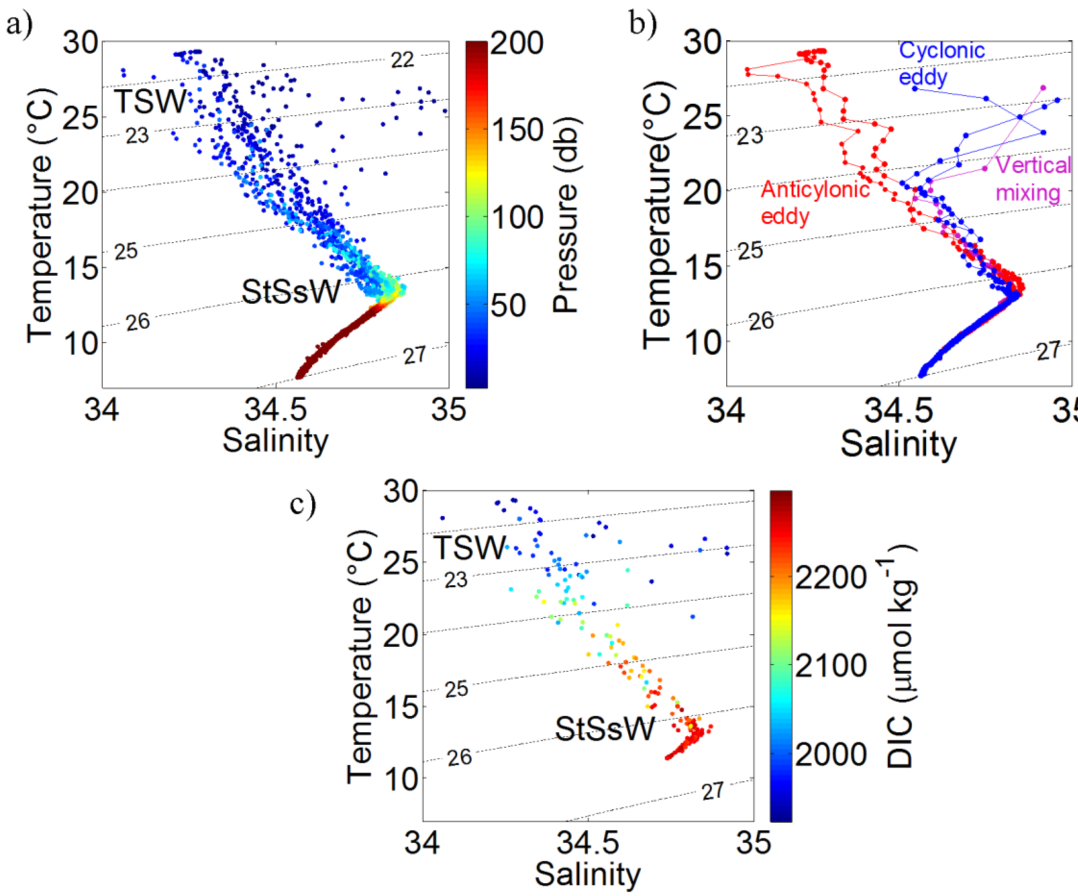

a)
TSW
StSsW
Temperature (°C)
Salinity
Pressure (db)
22
23
25
26
27
b)
Cyclonic eddy
Anticyclonic eddy
Vertical mixing
Temperature(°C)
Salinity
c)
TSW
StSsW
Temperature (°C)
Salinity
DIC (μmol kg^{-1})

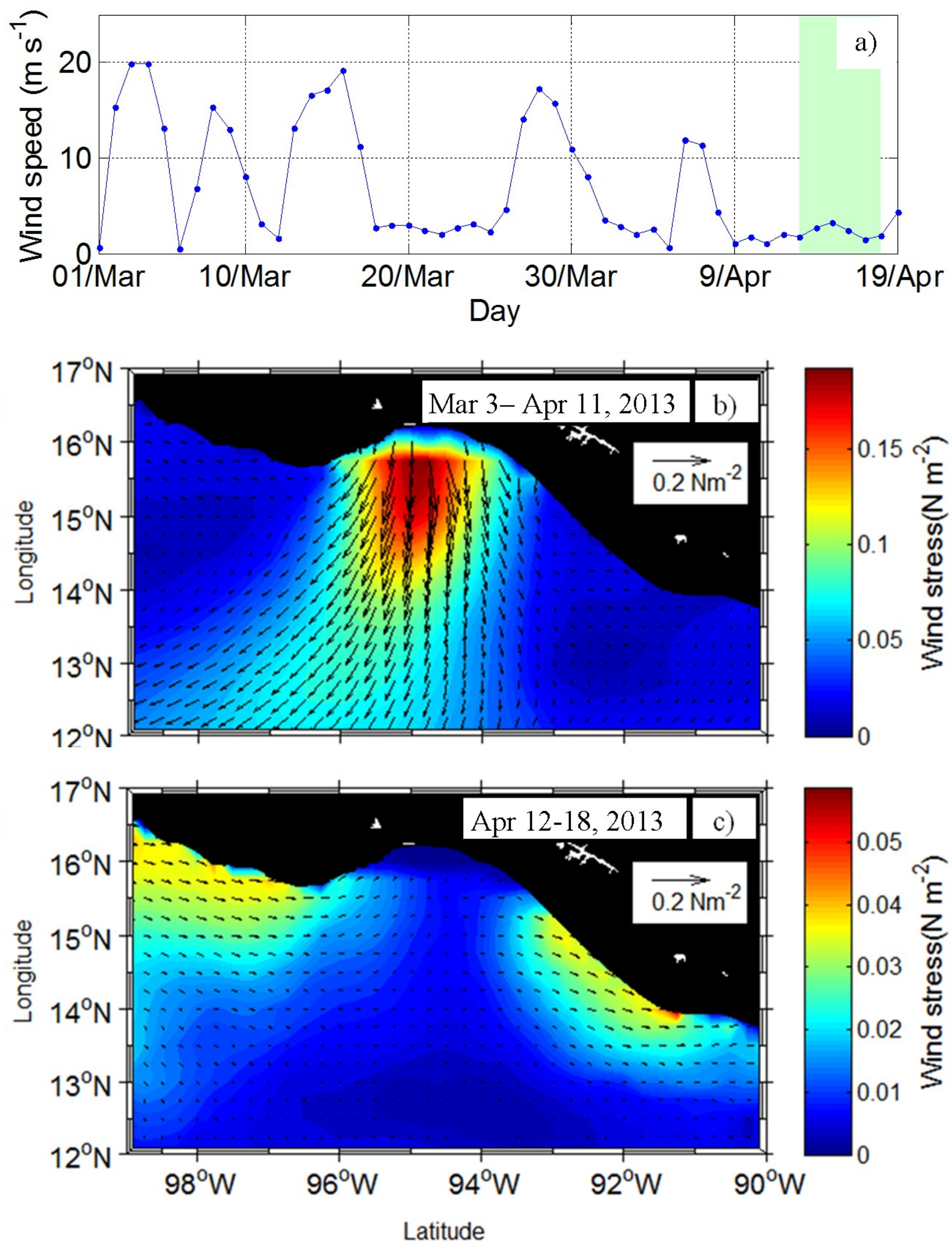

a)
Wind speed (m s^{-1})
Day
01/Mar
10/Mar
20/Mar
30/Mar
9/Apr
19/Apr
Mar 3– Apr 11, 2013
b)
0.2 Nm^{-2}
Wind stress(N m^{-2})
Longitude
Apr 12-18, 2013
c)
Latitude

1163

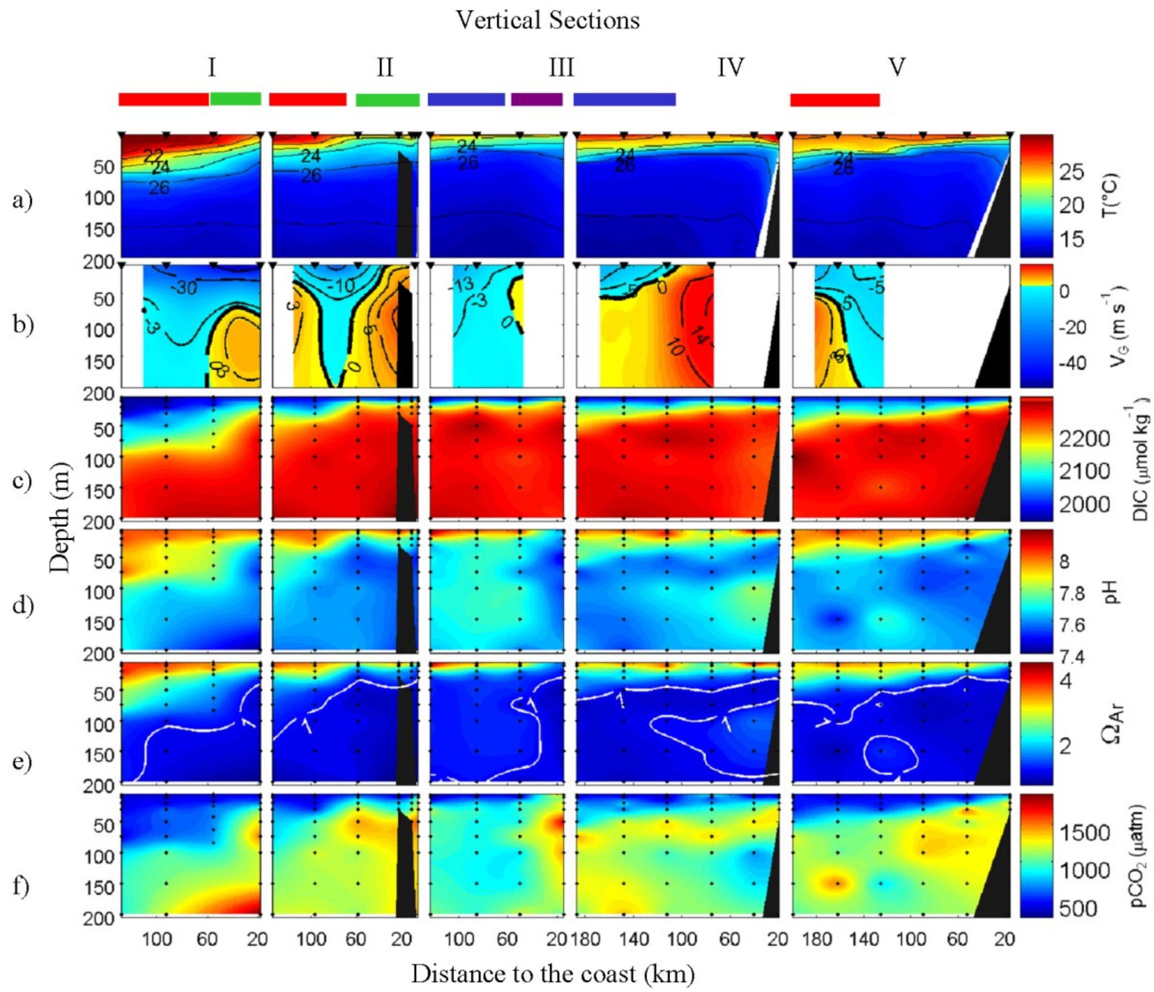
Vertical Sections
I
II
III
IV
V
a)
b)
c)
d)
e)
f)
Depth (m)
Distance to the coast (km)
T(°C)
V_G (m s^{-1})
DIC (μmol kg^{-1})
pH
Ω_{Ar}
pCO_2 (μatm)

[redacted]

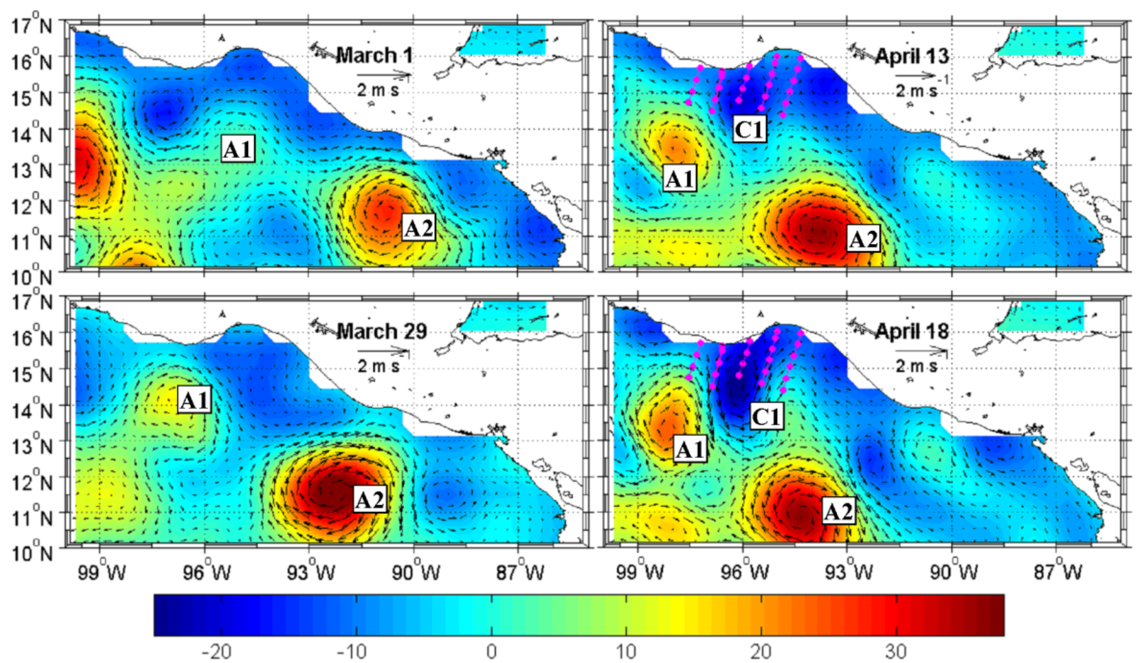
March 1
April 13
March 29
April 18
2 m s
A1
A2
C1
17°N
16°N
15°N
14°N
13°N
12°N
11°N
10°N
99°W
96°W
93°W
90°W
87°W
-20
-10
0
10
20
30

[redacted]

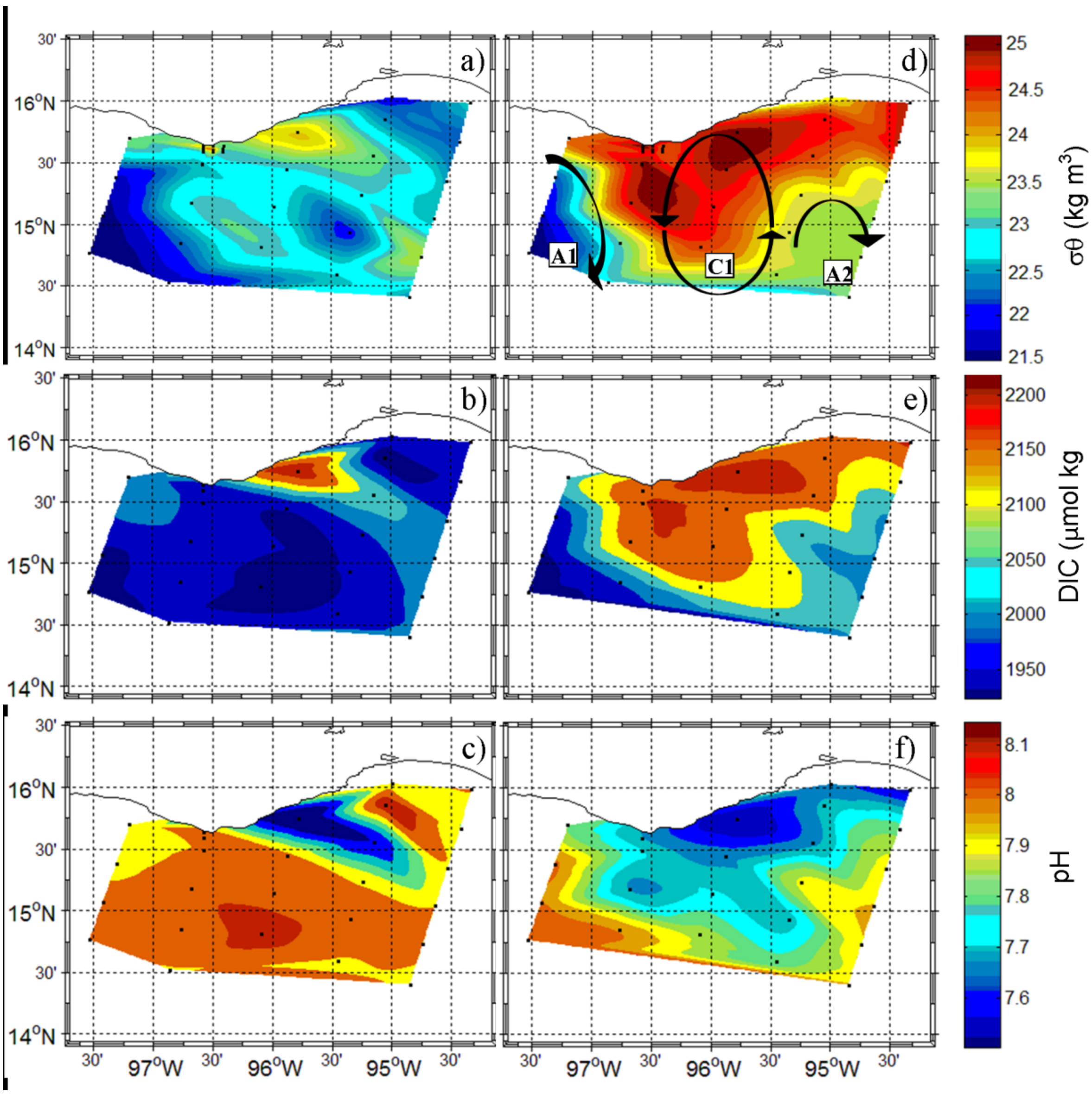

a)
b)
c)
d)
e)
f)
A1
C1
A2
σθ (kg m3)
DIC (µmol kg
pH
16°N
15°N
14°N
30'
97°W
96°W
95°W
25
24.5
24
23.5
23
22.5
22
21.5
2200
2150
2100
2050
2000
1950
8.1
8
7.9
7.8
7.7
7.6

1166

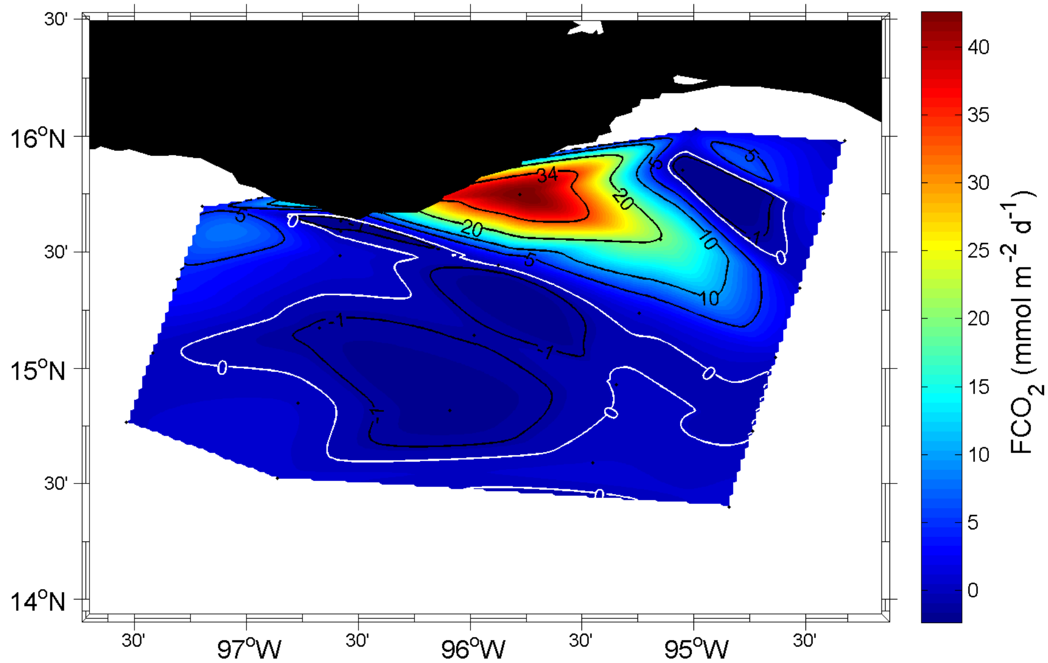

FCO2 (mmol m-2 d-1)
16°N
15°N
14°N
30'
97°W
96°W
95°W
0
5
10
15
20
25
30
35
40
34
20
10
-5
-1
0

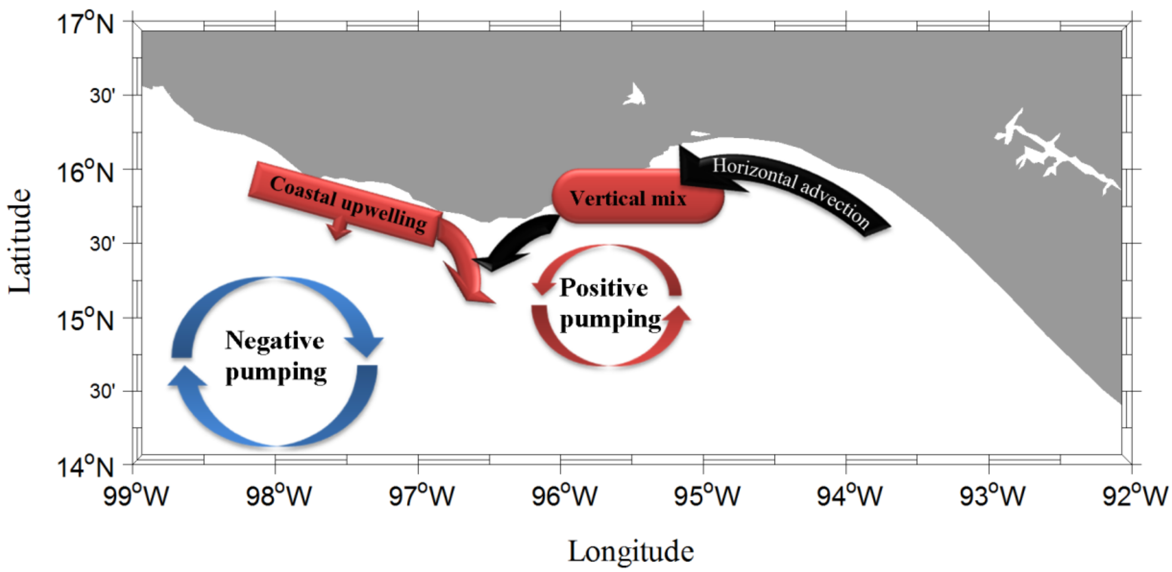

Latitude
Longitude
17°N
16°N
15°N
14°N
30'
99°W
98°W
97°W
96°W
95°W
94°W
93°W
92°W
Coastal upwelling
Vertical mix
Horizontal advection
Positive pumping
Negative pumping

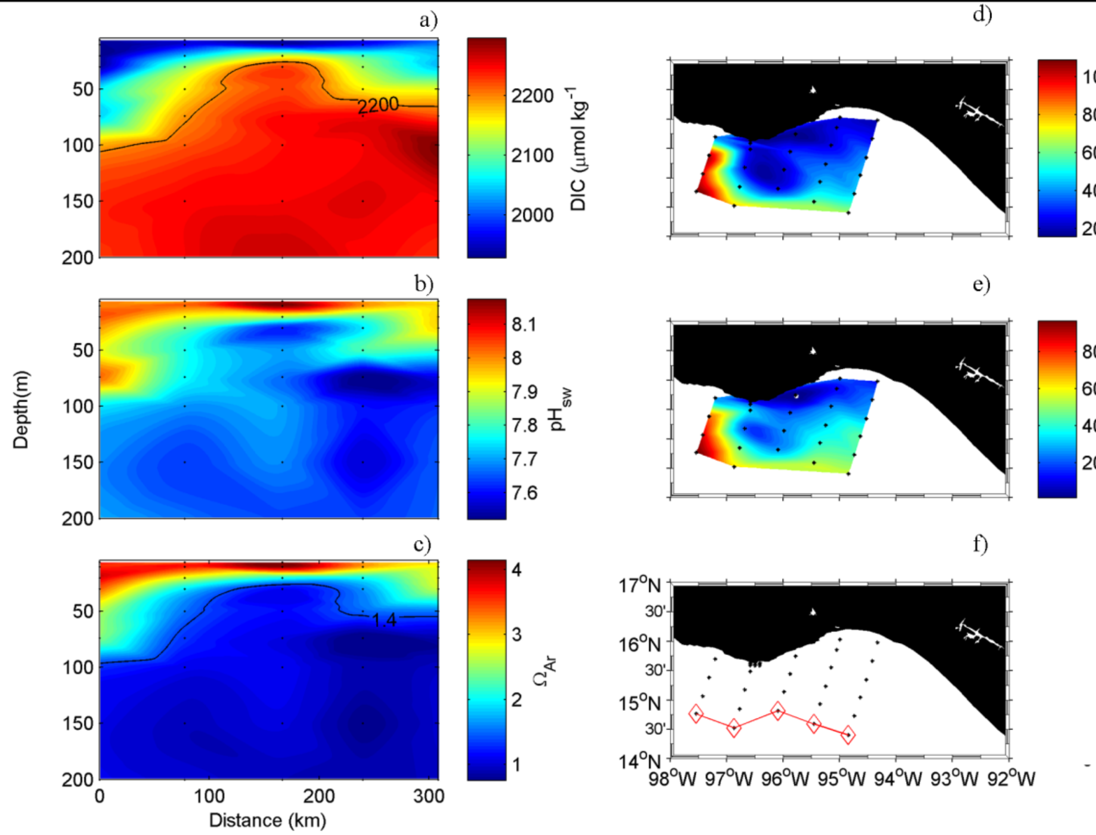

a)
b)
c)
d)
e)
f)
Depth(m)
Distance (km)
DIC (µmol kg⁻¹)
pH_{sw}
Ω_{Ar}
Depth (m)
2200
1.4
17°N
16°N
15°N
14°N
98°W 97°W 96°W 95°W 94°W 93°W 92°W